AD-A079 264 MARYLAND UNIV COLLEGE PARK INST FOR PHYSICAL SCIENCE--ETC F/G 12/1
RELIABLE ERROR ESTIMATION AND MESH ADAPTATION FOR THE FINITE EL--ETC(U)
APR 79 I BABUSKA , W C RHEINBOLDT N00014-77-C-0623
UNCLASSIFIED BBN-910 NL

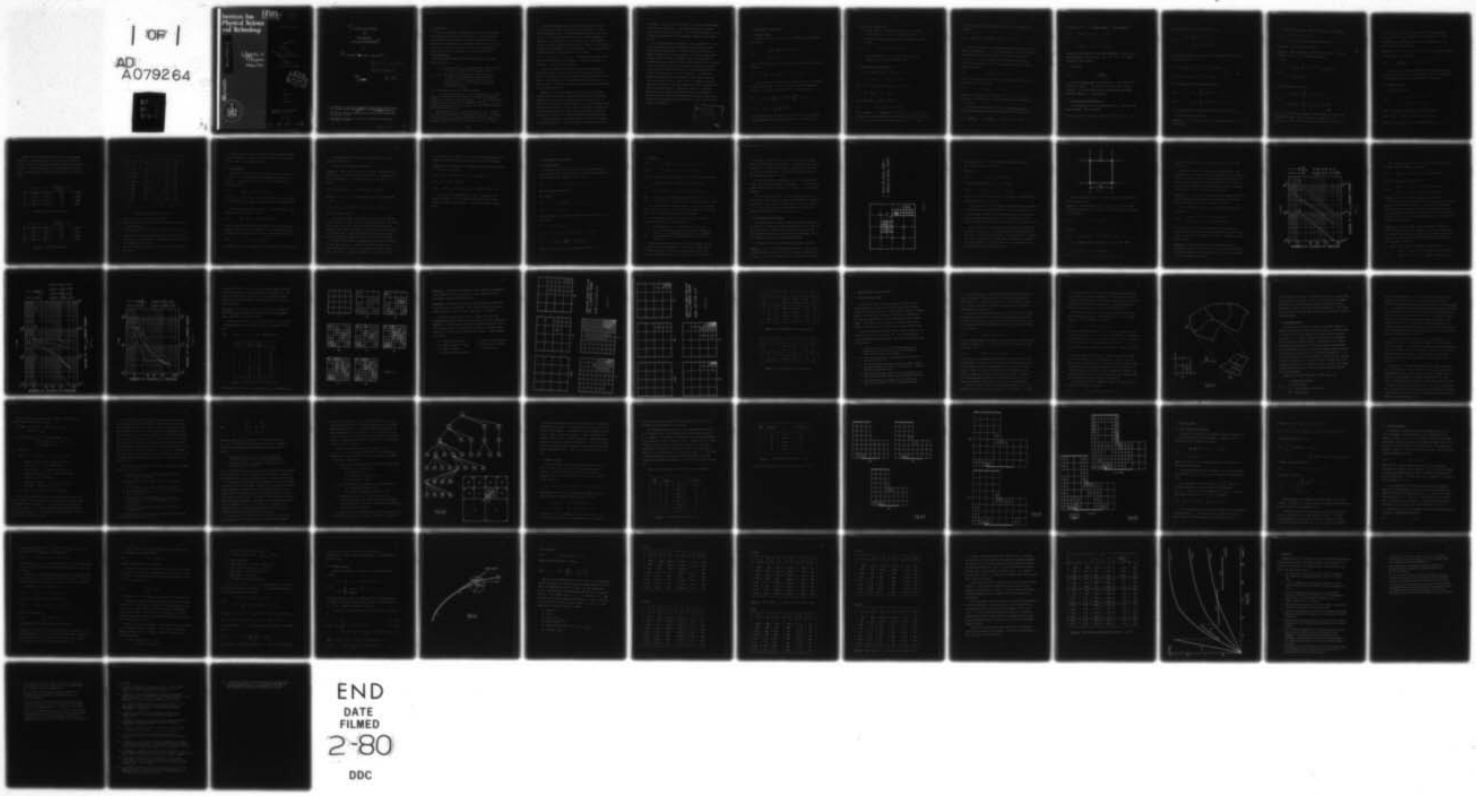

END
DATE
FILMED
2-80
DDC

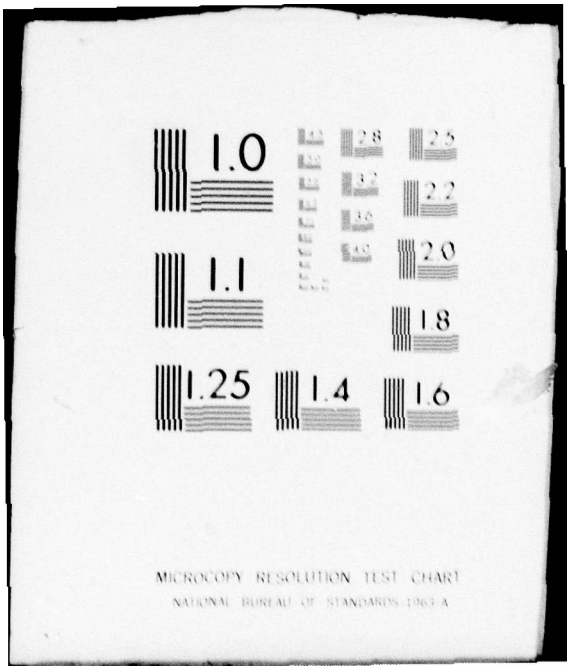
1.0
1.1
1.25
1.4
1.6
2.2
2.0
1.8
MICROCOPY RESOLUTION TEST CHART
NATIONAL BUREAU OF STANDARDS 1963 A

INSTITUTE FOR PHYSICAL SCIENCE AND TECHNOLOGY

LEVEL II

Technical Note BN-910

University of Maryland
College Park

Reliable Error Estimation and Mesh Adaptation for the Finite Element Method

by

I. Babuska

and

W. C. Rheinboldt

April 1979

(6) Reliable Error Estimation

and

Mesh Adaptation

for the Finite Element Method[1].

by

(10) Ivo Babuška[1,2] and Werner C. Rheinboldt[1,3]

(9) Technical note,

(14) BBN-910

(11) Apr[redacted]79

(12) 70

1) This work was in part supported under DOE Contract E(401)3443, NSF Grant MCS-78-05299, and ONR Contract N00014-77-C-0623.

(13) E(401)3443

2) Institute for Physical Science and Technology, University of Maryland, College Park, MD 20742

3) Department of Mathematics and Statistics, University of Pittsburgh, Pittsburgh, PA 15260

410 140 slb

1. Introduction

In the past two decades computational structural analysis and design have developed into very extensive subject areas. A major contributing factor certainly is the evolution of the finite element method into a powerful tool for the solution of a broad range of problems. In assessing trends for the future of these areas (see eg [1], [2], [3]) we need to take account of some of the questions for which there are as yet no satisfactory answers.

In this article we address two such questions which may be broadly phrased as follows:

(1.1)

(a) How can we calculate, at reasonable cost, reliable estimates of the error of computed finite element solutions?

(b) How should we set up the overall solution process so as to achieve, with reasonable certainty and efficiency, a solution for which the accuracy either falls into a prescribed range or is best possible for the allotted computational cost?

In this form both questions need further elaboration.

In practice, the accuracy of a finite element solution is usually measured in relation to the exact solution of the underlying mathematical problem, as for instance, an elasticity problem. In many instances there is interest also in the error of the mathematical model itself. In [1] we presented some comments on the latter question, but here we shall concentrate only on the first type of error.

Any measure of the accuracy involves the choice of a norm. Different norms show up different aspects of the error and in practice it is important to allow for a choice from among any reasonable collection of norms. This represents a demanding requirement on the design of the error estimates.

In practical engineering calculations the required accuracy usually is not very high; in fact, a range of 5-10% is often typical. In that case, the efficiency index Θ = error bound/exact error should satisfy, say, $1.0 \leq \Theta \leq 1.3$ for the bound to be realistic. For accuracies beyond, 10% the value of Θ may become worse but, on the other hand, Θ should tend to one when the accuracy becomes better and better. This points to the possibility of relaxing the requirement for a guaranteed bound. In fact, we may consider accepting estimates ε of the exact error $||e||$ for which

$\varepsilon/||e|| = 1 + O(||e||^{\alpha})$ as $||e|| \to 0$. Here the bound in the O-term need not be explicitly known but the exponent $\alpha > 0$ should be reasonable; for instance, $\alpha = 2$ would be rather desirable.

A-priori error bounds, as important as they are for the theory, are rarely very realistic for practical problems. Thus we have to consider a-posteriori estimates which utilize information obtained during the solution process. At the same time, such estimates open up the possibility of an adaptive control of the solution process itself to achieve the goal contained in the second question (1.1).

Generally, any overall assessment of the efficiency of the finite element solution of a practical problem should include not only the direct computational costs but also the expenses for data preparation, etc. A particularly costly part is here the construction of the finite element meshes which should be automatized as much as possible. Moreover, a solution with optimal accuracy within a given range of computational effort can hardly be achieved without the use of a responsive adaptive mesh-design algorithm.

Any efficient answer to the second question (1.1) can only be achieved by a complete integration of the error estimates and adaptive controls into

the software. For this, special attention has to be paid to data management and the overall program design. Here modern developments in computer science have to be taken into account. Thus a satisfactory answer to (1.1)(b) will have to integrate results from engineering, mathematics, and computer science.

In this paper we present some answers to the two questions (1.1). In [4]-[6] a mathematical theory of a-posteriori error estimates for finite element solutions has been given. Instead of discussing this theory in general we present here its principal aspects in the case of several model problems. More specifically, in Chapters 2 and 3 we consider certain one-dimensional and two-dimensional linear problems, respectively, and present a number of experimental results which show the effectivity of the bounds. From a theoretical viewpoint there are still various open questions which, in Chapter 3, are formulated as a list of conjectures. In Chapter 4 we summarize our current work on an experimental finite element solver which is aimed at answering question (1.1)(b). Finally, in Chapter 5 we give an extension of the results to nonlinear problems and of their integration with modern continuation techniques. Experimental results for a particular nonlinear two-point boundary value problem show that the combination of continuation, error estimation, and adaptive mesh construction should be an extremely effective approach to the computational solution of many practical problems in engineering.

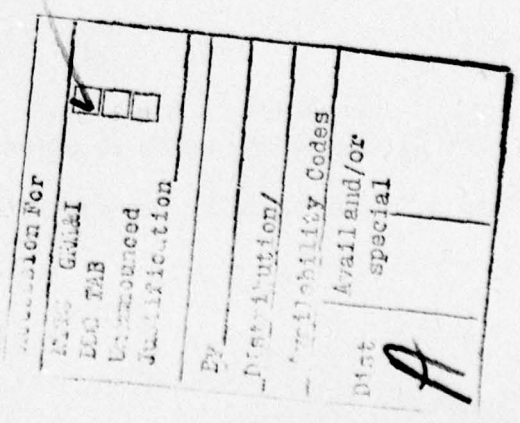

2. One-Dimensional Linear Problems

2.1 The Model Problem

On the unit interval $I = [0,1] \subset R^1$ we consider the elliptic boundary value problem

$$
\begin{aligned}
&-\frac{d}{dx}\left(a(x)\,\frac{du}{dx}\right) + b(x)u = f(x)\ ,\ x \in I\ ,\\
&u(0) = u(1) = 0
\end{aligned}
\tag{2.1}
$$

Specific smoothness conditions for a,b,f will be given later; but we require always that

$$
\bar{a} = \sup_{x\in I} < \infty\ ,\ \underline{a} = \inf_{x\in I} a(x) > 0\ ,\ \infty > \bar{b} \geq b(x) \geq 0,\ \forall x \in I \tag{2.2}
$$

As indicated in the Introduction, the problem formulation is incomplete without a specification of the norm to be used in measuring the desired accuracy. As an example, we consider the L_p-stress-energy norms.

$$
\|u\|_{E,p} = \left\{ \int_I [(a(u')^2)^{1/2}]^p \, dx \right\}^{1/p}\ ,\ \text{for } 1 \leq p < \infty \tag{2.3}
$$

$$
\|u\|_{E,\infty} = \sup_{x\in I} \left|(a(u')^2)^{1/2}\right|. \tag{2.4}
$$

Let u_0 denote the exact solution of (2.1), (2.2) and $u(\Delta)$ any approximate solution obtained by the finite element method for a given mesh Δ on I.

Then we have the following tasks:

(a) Compute reliable, close bounds of the error $||u_0 - u(\Delta)||_{E,p}$ under the norm (2.3), (2.4) with a specified value of p.

(b) Design an effective, adaptive algorithm to compute $u(\Delta)$ so that either

$$||u_0 - u(\Delta)||_{E,p} \leq \tau ||u_0||_{E,p} \tag{2.5}$$

for a given tolerance $\tau > 0$, or that $||u_0 - u(\Delta)||_{E,p}$ is minimal for a given total computational cost.

2.2 Error Indicators and Estimators - I

Let $P(\kappa)$ denote a family of partitions Δ of I,

$$\Delta: \ 0 = x_0^\Delta < x_1^\Delta < \ldots < x_m^\Delta = 1, \ m = m(\Delta),$$

$$I_j^\Delta = [x_{j-1}^\Delta, x_j^\Delta] \ , \ h_j^\Delta = x_j^\Delta - x_{j-1}^\Delta \ , \ j=1,\ldots, m(\Delta) \tag{2.6}$$

$$\overline{h}(\Delta) = \max_j h_j^\Delta \ , \quad \underline{h}(\Delta) = \min_j h_j^\Delta \ ,$$

which satisfy the κ-regularity condition

$$\underline{h}(\Delta) \geq c \, \overline{h}(\Delta)^\kappa \ , \quad \forall \Delta \in P(\kappa), \tag{2.7}$$

with a constant $c > 0$ independent of Δ. For each $\Delta \in P(\kappa)$ let $\overset{\circ}{S}{}^\Delta$ be the set of all continuous functions on I which are linear on each subinterval I_j^Δ, $j=1,\ldots, m(\Delta)$, and zero at the endpoints $x_0^\Delta = 0$, $x_m^\Delta = 1$. Then,

as usual, the finite element element solution $u(\Delta) \in \overset{\circ}{S}^{\Delta}$ is defined by the condition

$$(2.8) \qquad \int_0^1 [a\,u(\Delta)'\,v' + b\,u(\Delta)\,v]dx = \int_0^1 fv\,dx\ , \qquad \forall v \in \overset{\circ}{S}^{\Delta}.$$

We use a local analysis to construct estimates of the error $e(\Delta) = u_0 - u(\Delta)$ under any specified norm $||.||_{E,p}$. More specifically, from locally available information we compute an error indicator η_j^{Δ} for each mesh-interval I_j^{Δ}, $j=1,\ldots, m(\Delta)$. These indicators are then combined appropriately to yield an error estimator $\varepsilon(\Delta)$ which, in some sense, represents an approximation of the error:

$$(2.9) \qquad ||e(\Delta)||_{E,p} \backsim \varepsilon(\Delta).$$

Finally, again on the basis of the locally available data, we calculate an error corrector $\phi(\Delta)$ such that

$$(2.10) \qquad ||e(\Delta)||_{E,p} \leq \varepsilon(\Delta) + \phi(\Delta)$$

Note that in the evaluation of the quantities $\{\eta_j^{\Delta}\}$, $\varepsilon(\Delta)$, $\phi(\Delta)$ only information is to be used that is readily computable during the computation of $u(\Delta)$ itself.

The estimators and correctors are said to be <u>asymptotically exact</u> if, under reasonable assumptions about the solution and the partitions, we have

$$(2.11) \qquad \frac{\varepsilon(\Delta)}{||e(\Delta)||_{E,p}} \to 1\,, \quad \frac{\phi(\Delta)}{||e(\Delta)||_{E,p}} \to 0\,, \text{ as } \bar{h}(\Delta) \to 0,\ \Delta \in P(\kappa).$$

Furthermore, we call $\varepsilon(\Delta)$ an upper-estimator , or lower-estimator if

$$(2.12) \qquad ||e(\Delta)||_{E,p} \leq \overline{K}\, \varepsilon(\Delta) , \quad \forall \Delta \in P(\kappa),$$

or

$$||e(\Delta)||_{E,p} \geq \underline{K}\, \varepsilon(\Delta) , \quad \forall \Delta \in P(\kappa),$$

respectively, with constants $\overline{K},\underline{K}$ which are independent of Δ and $u(\Delta)$, but which may depend on other input data. Thus $\overline{\varepsilon}(\Delta) = \varepsilon(\Delta) + \phi(\Delta)$ always represents an upper-estimator.

The quotient

$$(2.14) \qquad \Theta = \frac{\varepsilon(\Delta)}{||e(\Delta)||_{E,p}}$$

is called the efficiency index of the estimator $\varepsilon(\Delta)$. As outlined in the Introduction, we want Θ to be as near to one as possible. Since, in practice, Θ is not available this means that we should analyse general conditions under which Θ approximates one.

2.3 Error Indicators and Estimators - II

For the problem (2.1), (2.2) we assume now that a', b, and f are p-th-power integrable. Then the residuals

$$(2.15) \quad r_j(x) = f(x) + a'(x)u(\Delta)'(x) - b(x)u(\Delta)(x), \quad \forall x \in I_j^{\Delta} , \; j=1,2,\ldots, m,$$

on the subintervals I_j^Δ belong to $L_p(I_j^\Delta)$. With

$$a_j = a(\tfrac{1}{2}(x_{j-1}^\Delta + x_j^\Delta))$$

(2.16)

$$\bar{r}_j = \int_{I_j^\Delta} r_j(x)(x-x_{j-1}^\Delta)(x_j^\Delta - x)dx$$

we introduce the following two types of error indicators for the norm (2.3) with some specified p, $1 < p < \infty$:

$$\left.\begin{aligned} (2.17)\quad \eta_j(\Delta) &= \tfrac{1}{2}(p+1)^{-1/p}\, a_j^{-1/2}\, h_j \left[\int_{I_j^\Delta} |r_j(x)|^p dx\right]^{1/p} \\ (2.18)\quad \hat{\eta}_j(\Delta) &= 3(p+1)^{-1/p}\, a_j^{-1/2}\, h_j^{-2+1/p}\, |\bar{r}_j| \end{aligned}\right\} \quad j=1,\ldots,m(\Delta)$$

The corresponding error estimators are defined by

$$(2.19)\qquad \varepsilon(\Delta) = \left[\sum_{j=1}^{m(\Delta)} \eta_j(\Delta)^p\right]^{1/p}, \quad 1 \le p < \infty$$

$$(2.20)\qquad \hat{\varepsilon}(\Delta) = \left[\sum_{j=1}^{m(\Delta)} \hat{\eta}_j(\Delta)^p\right]^{1/p}, \quad 1 \le p < \infty$$

It is readily seen how to define analogous quantities for the case $p=\infty$.

Then the following result holds:

Theorem 2.1: If $a', b, f \in L_p(I)$ then $\varepsilon(\Delta)$ is an upper-estimator and $\hat{\varepsilon}(\Delta)$ a lower-estimator.

Suppose that the smoothness conditions for a,b,f are strengthened to

(2.21)
$$\text{(i)}\quad a \in C^2(I),\ b,f \in C^1(I)$$
$$\text{(ii)}\quad u_0'' \text{ has only finitely many simple roots in } I;$$

then theorem 1 can be improved as follows:

Theorem 2.2: Under the smoothness conditions (2.21) and for $\Delta \in P(\kappa)$ the estimators $\varepsilon(\Delta)$ and $\hat{\varepsilon}(\Delta)$ are asymptotically exact.

With

(2.22)
$$\delta_j = \inf_t \sup_{x\in I_j} |a(x) - t| + \frac{1}{2} p^{-1/p} h_j \sup_{x\in I_j} |b(x)|,$$
$$\hat{r}_j = \frac{1}{h_j} \int_{I_j^\Delta} r_j(x)dx,$$

we now introduce the error corrector

(2.23)
$$\phi = C_1(p,\underline{a},\bar{a},\bar{b}) \left[\sum_{j=1}^{m(\Delta)} |\eta_j(\Delta)|^p \delta_j^p\right]^{1/p}$$
$$+ C_2(p,\underline{a},\bar{a},\bar{b}) \left[\sum_{j=1}^{m(\Delta)} h_j^p \int_{I_j} |r_j(x) - \hat{r}_j|^p dx\right]^{1/p}.$$

Here C_1, C_2 are constants dependent on p and the bounds (2.2) which can be estimated from above. Under our smoothness assumptions (2.21) the quantities δ_j are of order $\bar{h}(\Delta)$ and hence the first term of (2.23) is of

order $\varepsilon(\Delta)\ \bar{h}(\Delta)$. With the aid of the basic a-priori relation between $||e||_{H_p^1(I)}$ and $||e||_{H_p^0(I)}$ and because $u'(\Delta)$ is constant on I_j, it can be shown that also the second term of (2.23) is of the order $\varepsilon(\Delta)\ \bar{h}(\Delta)$. This leads to the following result:

Theorem 2.3: If $a', b, f \in L_p(I)$ then $\phi(\Delta)$ is an error corrector. Moreover, if the conditions (2.21) hold, then

$$\frac{\phi(\Delta)}{||e(\Delta)||_{E,p}} \to 0\ , \quad \text{as } \bar{h}(\Delta) \to 0,\ \Delta \in P(\kappa). \tag{2.24}$$

These are only some examples of possible error-indicators, estimators, and correctors which have the desired properties. There is no unique form for these quantities and various other definitions are possible.

2.4 A Numerical Example

We consider the problem

$$\begin{aligned} &-((x+t)^{1/10}\ u')' + u = f(x) \\ &u(0) = u(1) = 0, \quad t = \frac{1}{10}\ , \end{aligned} \tag{2.25}$$

where f is chosen such that the exact solution has the form

$$u_0(x) = (x+t)^{1/2} - [(1-x)t^{1/2} + x(1+t)^{1/2}],\ x \in I. \tag{2.26}$$

This allows us to compute here the efficiency index (2.14).

Tables 2.1 and 2.2 below show the errors in the L_2- and L_8-norm, respectively, for uniform partitions on I with $h = 1/20$, $h = 1/40$, and $h = 1/80$, as well as for the non-uniform partitions 20A with $m = 20$ given in Table 2.3. The error indicators (2.17) and estimators (2.19) were used. The partitions 20A are optimal in the sense defined in Section 2.5 below.

	$\|\|e\|\|_{E,2}$	$\varepsilon(\Delta)$	$\frac{\|\|e\|\|_{E,2}}{\|\|u_0\|\|_{E,2}} \cdot 100$	Θ
20	.2287(-1)	.2313(-1)	3.22%	1.01168
40	.1156(-1)	.1159(-1)	1.62%	1.00309
80	.5796(-2)	.5801(-2)	.809%	1.00076
$20A_2$	.1268(-1)	.1270(-1)	1.77%	1.00177

Table 2.1: Errors under the L_2-norm

	$\|\|e\|\|_{E,8}$	$\varepsilon(\Delta)$	$\frac{\|\|e\|\|_{E,8}}{\|\|u_0\|\|_{E,8}} \cdot 100$	Θ
20	.6933(-1)	.7569(-1)	4.79%	1.09174
40	.3647(-1)	.3198(-1)	2.42%	1.04975
80	.1855(-1)	.1922(-1)	1.21%	1.03632
$20A_8$	.1861(-1)	.1931(-1)	1.22%	1.03778

Table 2.2: Errors under the L_8-norm

j	x_j^Δ		j	x_j^Δ	
	p=2	p=8		p=2	p=8
0	0	0	10	.2397	.1705
1	.1326(-1)	.9155(-2)	11	.2828	.2042
2	.2822(-1)	.1942(-1)	12	.3312	.2435
3	.4508(-1)	.3096(-1)	13	.3856	.2895
4	.6408(-1)	.4398(-1)	14	.4465	.3438
5	.8546(-1)	.5873(-1)	15	.5148	.4083
6	.1095	.7547(-1)	16	.5913	.4854
7	.1336	.9456(-1)	17	.6769	.5783
8	.1670	.1164	18	.7228	.6910
9	.2012	.1415	19	.8800	.8291
			20	1	1

Table 2.3: The non-uniform meshes 20A.

These results suggest the following observations:

(a) For uniform partitions the asymptotic decrease of the error is linear in h under both norms.

(b) For the L_2-norm the efficiency index θ converges to 1 with $||e||^2_{E,2}$.

(c) The efficiency index improves with decreasing relative error and, in particular, it is better for the non-uniform optimal partitions than for the corresponding uniform ones.

(d) The error estimators are more effective under the L_2-norm than under the L_8-norm.

Observations such as these are typical for much more general problems than the present one. In particular, as we shall see in the next chapter, they also apply to the two-dimensional case.

2.5 Optimal Meshes

We restrict our consideration now to a special class of partitions. For this let $\xi \in C^1(I)$ be any strictly increasing function with $\xi(0) = 0$ and $\xi(1) = 1$. Then a partition (2.6) is called a (ξ,m)-partition and denoted by $\Delta(\xi,m)$ if

$$\xi(x_j^{\Delta}) = \frac{j}{m} \quad , \; j=0,1,\ldots, \; m = m(\Delta). \tag{2.27}$$

The set of all (ξ,m)-partitions $\Delta(\xi,m)$ associated with a fixed ξ and varying m is called the family of graded partitions induced by the grading function ξ.

For such families of graded partitions it is possible to show -- under suitable conditions on u_0 and ξ -- that

$$\lim_{m\to\infty} m||e||_{E,p} = \omega(p, u_0, \xi)(1 + o(1)). \tag{2.28}$$

This will allow us to associate with every member $\Delta(\xi,m)$ of the family the asymptotic error $\omega(p, u_0, \xi)/m$. Moreover, it turns out that there exists a grading function ξ_0 such that for all other grading functions ξ we have

$$\omega(p, u_0, \xi_0) \leq \omega(p, u_0, \xi). \tag{2.29}$$

This means that ξ_0 induces an asymptotically optimal family of graded partitions.

Our discussion here will be restricted to the case $p = 2$. For all details we refer to [6].

The basic result may be phrased as follows:

Theorem 2.4: Suppose that the conditions (2.21) hold. Then there exists a grading function ξ_0 such that $\Delta(\xi_{0,m}) \in P(\frac{5}{3})$ for all $m \geq 1$ and that for any other grading function $\xi \neq \xi_0$ for which $\Delta(\xi,m) \in P(\kappa)$ for some $1 \leq \kappa < 2$ we have

$$(2.30) \quad ||e(\Delta(\xi_{0,m}))||_{E,2} < ||e(\Delta(\xi,m))||_{E,2}, \quad \forall m \geq m_0(\xi).$$

Moreover, if $\xi = \xi_0 + \lambda\phi$ is a grading function for all sufficiently small λ then

$$(2.31) \quad ||e(\Delta(\xi_0 + \lambda\phi, m))||_{E,2} < ||e(\Delta(\xi_0, m))||_{E,2} + O(\lambda^2), \text{ as } \lambda \to \infty$$

for all sufficiently large m.

In most practical problems the optimal partition is rather sensitive to small changes of the data. But (2.31) shows that the optimal error changes only with the square of any change of the optimal partition and hence is considerably more stable than the latter. In other words, there is no reason why we should attempt to compute the optimal partition at high cost when near-optimal partitions produce almost the same error as the optimal one.

The optimal grading function ξ_0 depends on u_0 and p and is not difficult to obtain when u_0 is known. In fact, the partitions of Table 2.3 are $(\xi_0, 20)$-partitions for (2.25) and were computed from the exact solution (2.26). The table clearly shows the dependence of ξ_0 on the value of p.

In general, when u_0 is unknown, it turns out that we may approximate ξ_0 by means of the following equilibration principal for the error indicators:

Theorem 2.5: Let the conditions (2.21) hold and suppose that for some family T of partitions (2.6) we have

$$(2.32)\quad \eta_j(\Delta) = \mu(1 + \mathcal{O}(\bar{h}(\Delta)^\rho), j = 1,\ldots,m(\Delta), \text{ as } \bar{h}(\Delta) \to 0,\ \Delta \in T,$$

with $\rho = 1/12$. Then $T \subset P(\frac{5}{3})$ and

$$(2.33)\quad ||e(\Delta)||_{E,2} \leq ||e(\Delta(\xi_0,m))||_{E,2}\ (1 + \mathcal{O}(\bar{h}(\Delta)^\rho), \text{as } \bar{h}(\Delta) \to 0,\ \Delta \in T.$$

From a practical viewpoint theorems 2.4 and 2.5 suggest the use of adaptive techniques for the simultaneous construction of nearly optimal partitions and their error estimators. This will be discussed in Chapter 4 below.

3. Two-Dimensional Linear Problems

3.1 The Model Problems

As before, for simplicity of discussion we present the results for certain model problems. More specifically, we consider the following two elliptic boundary value problems on the unit square

$$\Omega = \{x_1, x_2 \in R^2 \mid 0 < x_1, x_2 < 1\} \tag{3.1}$$

with Dirichlet boundary conditions:

(a) Problem L:

$$\Delta u + p \frac{\partial^2 u}{\partial x \partial y} = 0, \quad \text{on} \quad \Omega, \; 0 \leq p < 2 \tag{3.2}$$

$$u = g \ , \ \text{on} \quad \partial\Omega \tag{3.3}$$

Here the function g is chosen such that the exact solution of (3.2), (3.3) is given by

$$u_0 = r^{1/2} \cos \theta/2$$

$$r = \left[\frac{1}{2+p} (x_1 - t + x_2)^2 + \frac{1}{2-p} (x_1 - t - x_2)^2 \right]^{1/2} \tag{3.4}$$

$$\theta = \arctan \left(\sqrt{\frac{2+p}{2-p}} \ \frac{x_1 - t - x_2}{x_1 - t + x_2} \right), \; t > 1.$$

Hence for $p = 0$, r and θ are polar coordinates centered at $(t,0)$.

(b) Problem E:

$$\nabla^2 \underline{u} + \frac{1}{1-2\sigma} \nabla \cdot \nabla \underline{u} = 0 \quad \text{on } \Omega, \quad \underline{u} = (u_1, u_2), \tag{3.5}$$

$$\underline{u} = \underline{g}, \text{ on } \partial\Omega, \ 0 \leq \sigma < \frac{1}{2}, \ \underline{g} = (g_1, g_2). \tag{3.6}$$

Here $\underline{g}$ is chosen such that the exact solution of (3.5), (3.6) is as follows:

$$\begin{aligned} u_1 &= \frac{1}{2} r^{1/2}\left[(\kappa-1)\cos\frac{\theta}{2} - (\kappa-1)\sin\frac{\theta}{2} - \frac{1}{2}\cos\frac{3}{2}\theta - \frac{1}{2}\sin\frac{3}{2}\theta\right] \\ u_2 &= \frac{1}{2} r^{1/2}\left[(\kappa+1)\cos\frac{\theta}{2} + (\kappa+1)\sin\frac{\theta}{2} + \frac{1}{2}\cos\frac{3}{2}\theta - \frac{1}{2}\sin\frac{3}{2}\theta\right], \end{aligned} \tag{3.7}$$

where $\kappa = 3-4\sigma$ and r,θ are the polar coordinates centered at $(t,0)$, $t > 1$. For $t \to 1$ the solution has a singularity with a character typical for a corner.

Both problems have two parameters, namely, t,p in the case of problem L and t,σ in that of problem E. Here t controls the regularity of the solution while p and σ characterize the degeneracy of the problems.

We use admissible partitions Δ of the unit square (3.1) which are defined recursively by the following two rules:

(i) The undivided square is an admissible partition of itself.

(ii) If Δ is an admissible partition of (3.1) and s represents any square of Δ, then a new admissible partition Δ' is obtained if s is subdivided into four congruent squares of half the side-length of s. (3.8)

On these admissible partitions we use the finite element method with test function which are continuous on $\overline{\Omega}$ and bilinear on each square of Δ. Besides the usual nodal points, here called regular points, these partitions contain nodal points inside Ω which are not in the corner of

all the squares incident with them. These points are called irregular points and are marked by an x in Figure 3.1. Since the test functions are continuous on $\bar{\Omega}$, their values at these irregular points are not free but are specified by continuity. For instance, the value at point B is the average of the values at C and D.

As usual, with any regular nodal point, say "i", we associate the standard basis function and denote its support by Ω_i. For instance, the support associated with the nodal point A of Figure 3.1 is the indicated shaded set.

For any admissible partition Δ let the irregularity index $\chi(\Delta)$ be defined as the maximal number of irregular points between any two adjacent regular points. For instance, for the partition of Figure 3.1 we have $\chi(\Delta) = 4$. We shall always restrict our consideration to a family P of admissible partitions with $\chi(\Delta) \leq \bar{\chi} < \infty$ for all $\Delta \in P$.

3.2 Error Indicators and Estimators

For two-dimensional problems the theory of a-posteriori estimates is not yet as fully developed as for the one-dimensional case. We shall not go into the details of the theory here but indicate only some of the typical theorems and present certain representative experimental results. As in Chapter 2 we shall use the L_p-stress-energy norms.

The basic result may be broadly phrased as follows (see eg [4]):

Theorem 3.1: Let $\Delta \in P$ be an admissible partition on Ω and $u(\Delta)$ the corresponding finite element solution. For each regular nodal point i of Δ define $z_i \in H^1(\Omega_i)$ as the exact solution of the given problem on the

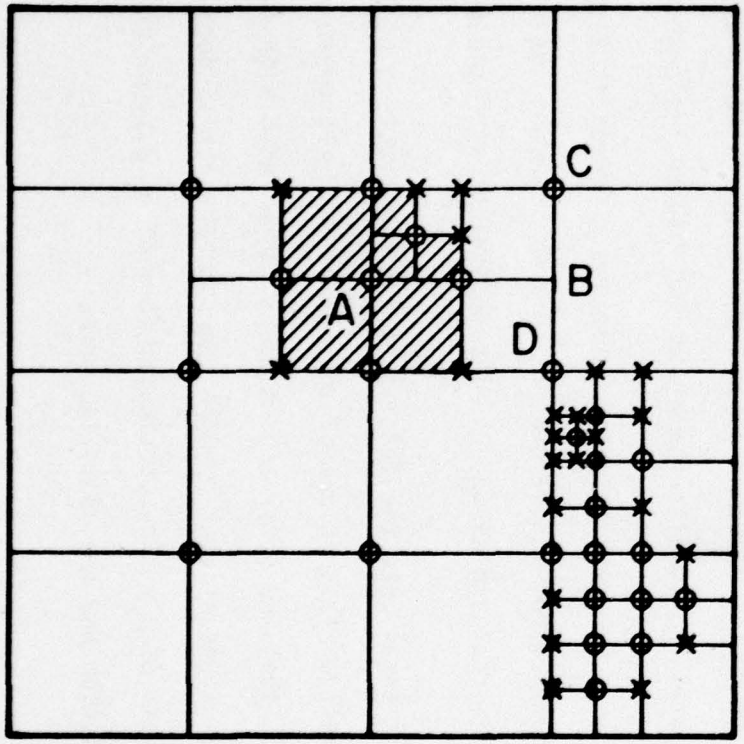

o REGULAR NODAL POINTS

× IRREGULAR NODAL POINTS

FIGURE 3.1

associated support set Ω_i which satisfies the boundary conditions $z_i = u(\Delta)$ on $\partial\Omega_i$ and $z_i = g$ on $\partial\Omega_i \cap \partial\Omega$.

Moreover, set

$$\tilde{\eta}_i = ||z_i - u(\Delta)||_{E,2,\Omega_i} . \tag{3.9}$$

Then there exist constants $K_2 \geq K_1 > 0$ such that

$$K_1||e||^2_{E,2,\Omega} \leq \sum_i \tilde{\eta}_i^2 \leq K_2||e||^2_{E,2,\Omega} \tag{3.10}$$

where $e = u_0 - u(\Delta)$ is the actual error. The constants K_1, K_2 depend on the problem and P, but not on Δ and $u(\Delta)$.

This shows that once again an upper- and lower-estimator can be obtained on the basis of strictly local information. Of course, in practice the $\tilde{\eta}_i$ are not computable. However, by using appropriate bounds it is possible to construct computable error indicators η_j for the elements of Δ which provide estimators that are asymptotically equivalent with the estimate (3.10).

We shall not enter into the details of the construction of these error indicators. Briefly, if s_i is one of the elements of the given partition (see Figure 3.2), then the error indicator η_i associated with s_i is composed of h_i and of the values of $u(\Delta)$ and the jumps of the normal derivatives of $u(\Delta)$ at the corners of s_i. The particular form of η_i depends only on the differential equation and the specified norm.

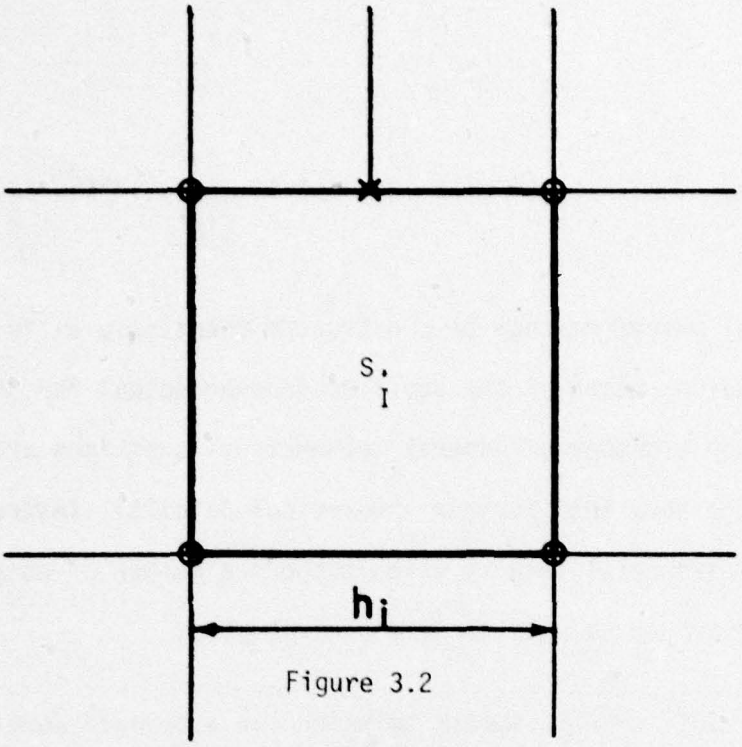

Figure 3.2

The basic asymptotic property of these indicators can be seen from the following special result:

Theorem 3.2: Let the domain be all of R^2. Then, for a family of uniform partitions with side-length $h(\Delta)$ and for sufficiently smooth exact solutions u_0, the estimator

$$\varepsilon(\Delta) = \left[\sum_i \eta_i^2 \right]^{1/2} \tag{3.11}$$

satisfies

$$||u_0 - u(\Delta)||_{E,2}^2 = \varepsilon(\Delta)^2 + O(h(\Delta)^4), \quad \text{as } h(\Delta) \to 0. \tag{3.12}$$

In all reasonable cases we expect that $||e||_{E,2} \geq Ch(\Delta)$, whence

$$\begin{aligned} ||u_0 - u(\Delta)||_{E,2} &= \varepsilon(\Delta)(1 + O(h(\Delta)^2)), \\ &= \varepsilon(\Delta)(1 + O(\varepsilon(\Delta)^2)), \text{ as } h(\Delta) \to 0. \end{aligned} \tag{3.13}$$

Hence the efficiency index (2.14) will converge to one with the square of the error.

Nearby optimal meshes may now be constructed adaptively as in the one-dimensional case by means of the equilibration-principal for the error-indicators. Because a number of general mathematical questions are still open, we will not go here into further theoretical details. Instead we present various experimental results which support a number of conjectures for which there is as yet no sufficiently general proof.

Conjecture 1: For sufficiently smooth solutions on a bounded domain and for uniform partitions, the efficiency index with respect to the L_2-stress energy norm converges to one with the square of the error.

This is clearly seen in Figure 3.3 for the solution of problem E in the two cases

$$\begin{aligned} &\text{case } E_1: \quad t = 2.0 \quad \sigma = 0.0, \text{ uniform partition,} \\ &\text{case } E_2: \quad t = 2.0\,, \sigma = 0.45, \text{ uniform partition.} \end{aligned} \tag{3.14}$$

The figure shows in log/log-scale the square of the error (under the L_2-stress energy norm) as well as the deviation from one of the efficiency index Θ as a function of the number N° of degrees of freedom of the finite element solution.

Conjecture 2: For uniform partitions on bounded domains the rate of convergence of the efficiency index to one is more strongly influenced by the smoothness properties of the exact solution u_0 than by the convergence of the finite element solutions to u_0.

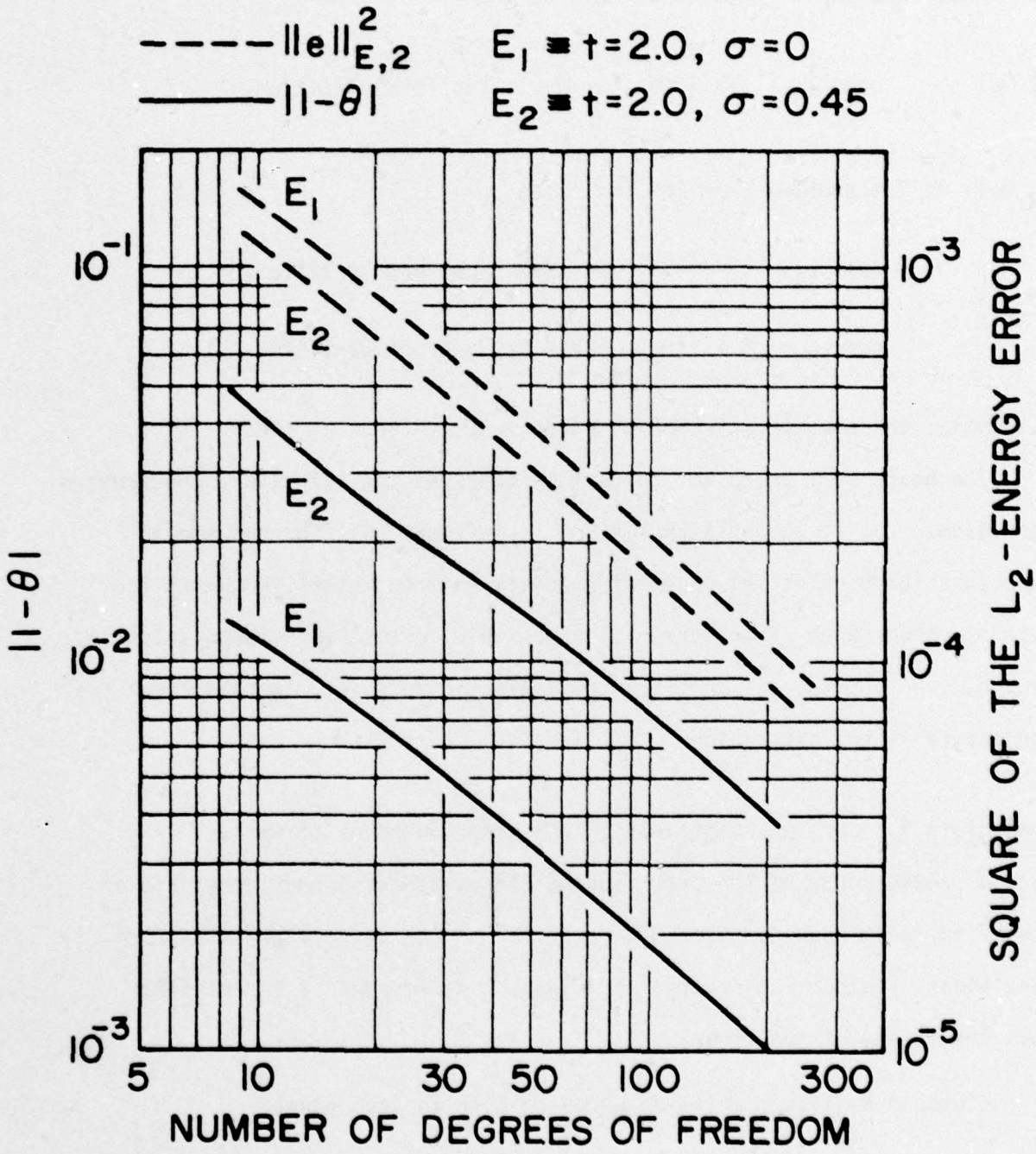
$\|e\|^2_{E,2}$
$|1-\theta|$
$E_1 \equiv t=2.0, \sigma=0$
$E_2 \equiv t=2.0, \sigma=0.45$
E_1
E_2
E_2
E_1
10^{-1}
10^{-2}
10^{-3}
10^{-3}
10^{-4}
10^{-5}
$|1-\theta|$
SQUARE OF THE L_2-ENERGY ERROR
5
10
30
50
100
300
NUMBER OF DEGREES OF FREEDOM

FIGURE 3.3

This is supported by Figure 3.4. It has the same form as Figure 3.3 and shows results for problem E, case E_1 and

(3.15) case E_3: $t = 1.05$, $\sigma = 0.0$, uniform partition,

as well as for problem L in the two cases

(3.16)
case L_1: $t = 1.05$, $p = 0.0$, uniform partition,
case L_2: $t = 1.001$, $p = 0.0$, uniform partition.

Evidently, the singularity becomes stronger as t tends to one.

The next, very important conjecture concerns the adaptively constructed partitions. Under suitable conditions it is known that for non-smooth solutions there exist sequences of properly refined meshes for which the rate of convergence of the error is comparable to that for smooth solutions, provided, of course, the same type of elements are used. In this light the conjecture is not surprising:

Conjecture 3: For the adaptively constructed sequences of meshes the rate of convergence of the error (under the L_2-stress energy norm) and of the efficiency index compares with that for smooth solutions and uniform partitions. In particular, the efficiency index converges essentially with the square of the error.

Figure 3.5 gives results for problem L in the two cases

(3.17)
case L_3: $t = 1.05$, $p = 0.0$, adaptively refined partition,
case L_4: $t = 1.05$, $p = 0.0$, adaptively refined partition.

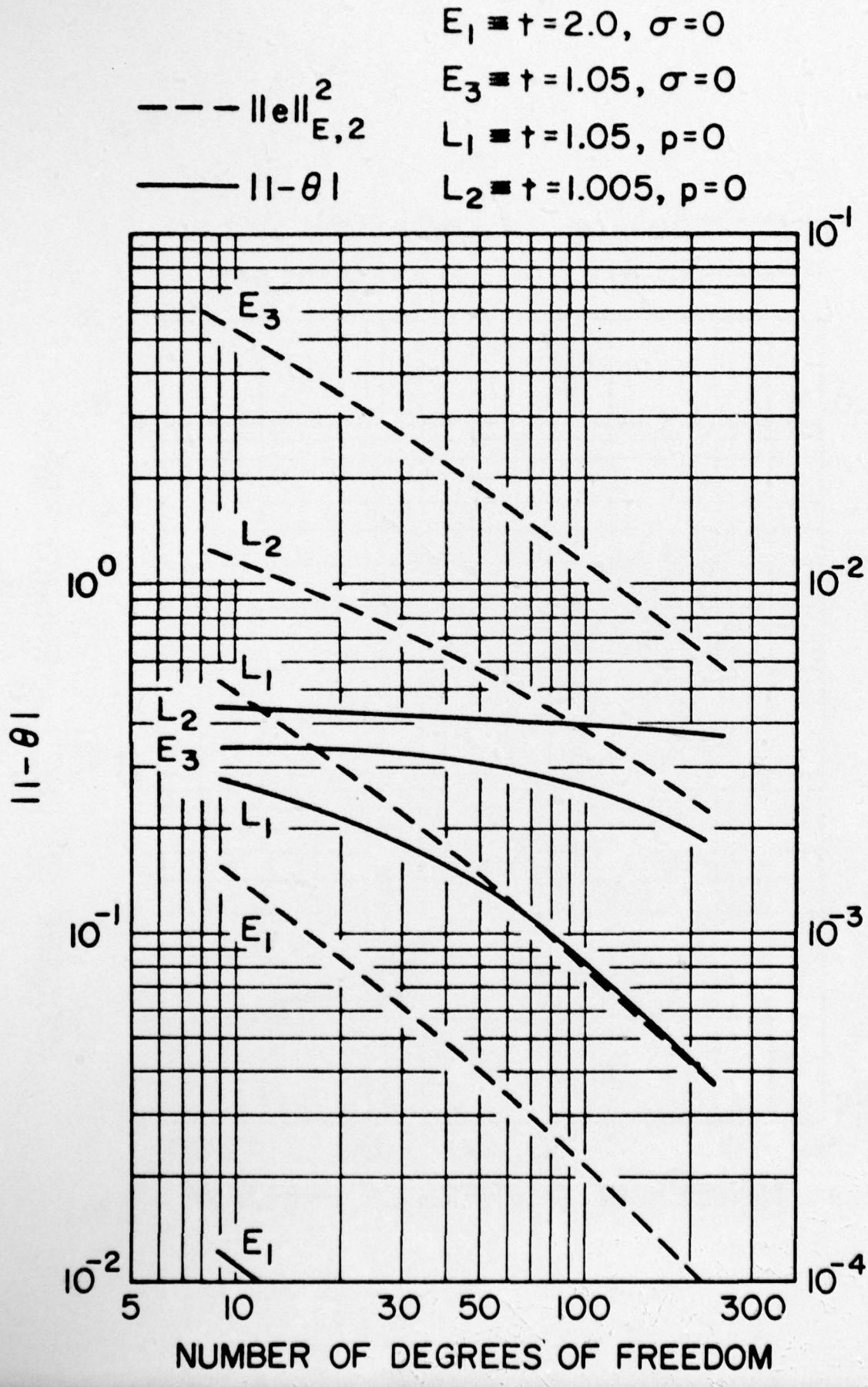
$E_1 \equiv t=2.0, \sigma=0$
$E_3 \equiv t=1.05, \sigma=0$
$L_1 \equiv t=1.05, p=0$
$L_2 \equiv t=1.005, p=0$
$\|e\|^2_{E,2}$
$|1-\theta|$
10^0
10^{-1}
10^{-2}
10^{-1}
10^{-3}
10^{-4}
5
10
30
50
100
300
NUMBER OF DEGREES OF FREEDOM
SQUARE OF THE L_2-ENERGY ERROR

FIGURE 3.4

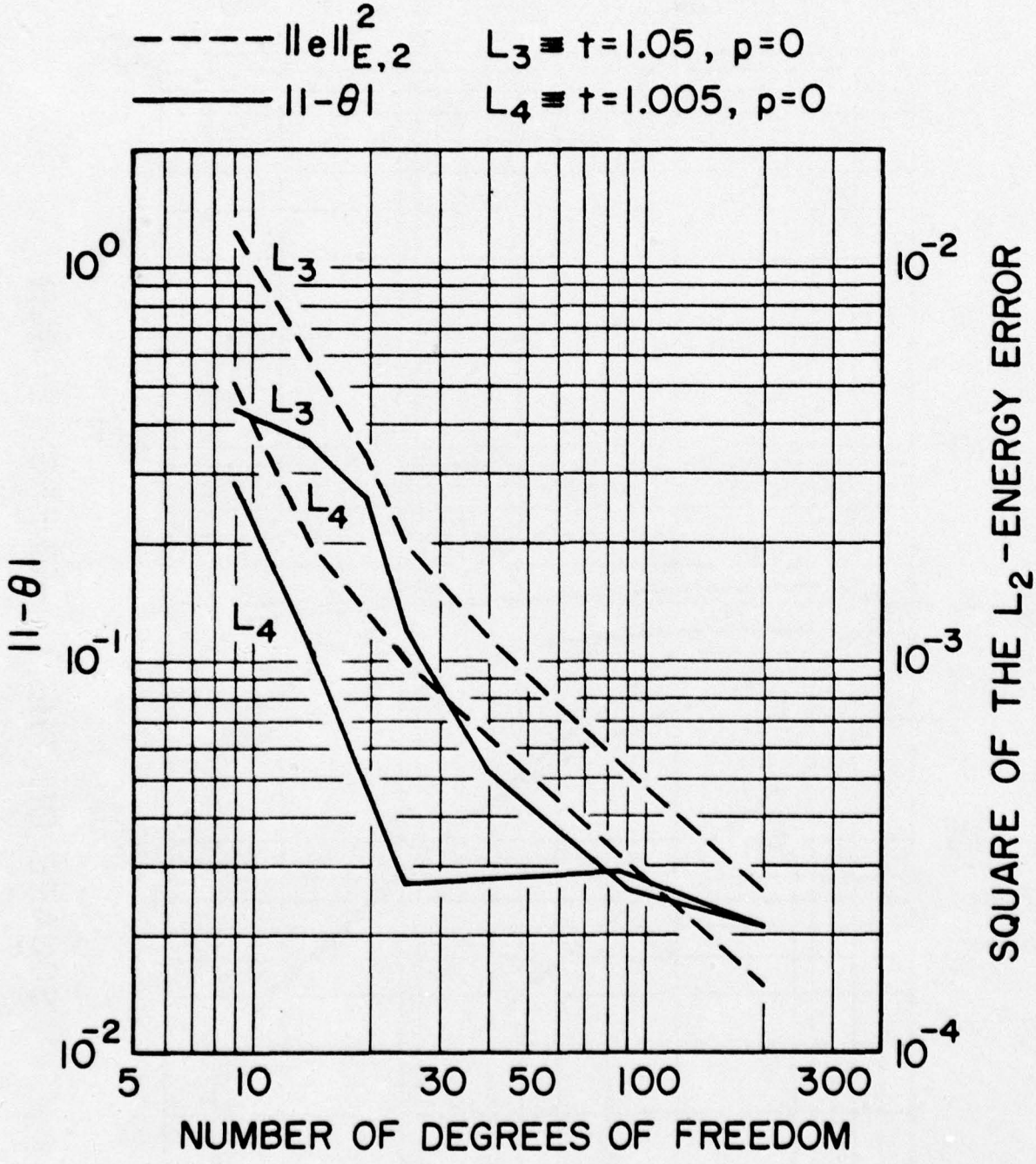
$\|e\|^2_{E,2}$
$|1-\theta|$
$L_3 \equiv t=1.05,\ p=0$
$L_4 \equiv t=1.005,\ p=0$
10^0
10^{-1}
10^{-2}
10^{-2}
10^{-3}
10^{-4}
L_3
L_3
L_4
L_4
5
10
30
50
100
300
NUMBER OF DEGREES OF FREEDOM
$|1-\theta|$
SQUARE OF THE L_2-ENERGY ERROR

FIGURE 3.5

A comparison of Figure 3.4 and 3.5 shows the contrast between the solution of the same problem using uniform-and adaptively-refined partitions. The behavior of the efficiency index close to one is influenced by various factors and is not fully understood. Some aspect of this is the topic of the next conjecture.

Conjecture 4: For completely arbitrary partitions of fixed irregularity index the efficiency index does not converge to one but has reasonable bounds, dependent on the requlrity index.

The partitions of Figure 3.6 were randomly generated. The conjecture is certainly supported by the results of Table 3.1 for problem L in the case

(3.18) case L_5: $t = 2.0$, $p = 0.0$, random partitions.

Partition	No of nodes	No of elements	Θ
1	9	16	.976
2	21	40	.868
3	34	64	.871
4	49	88	.868
5	72	115	.926
6	103	166	.901
7	121	190	.894
8	132	214	.877

Table 3.1 Efficiency indices for random partitions

As before the efficiency index Θ was computed under the L_2-stress-energy norm.

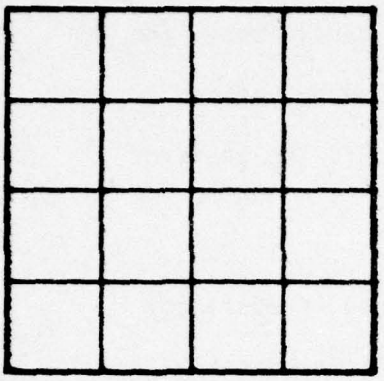

1

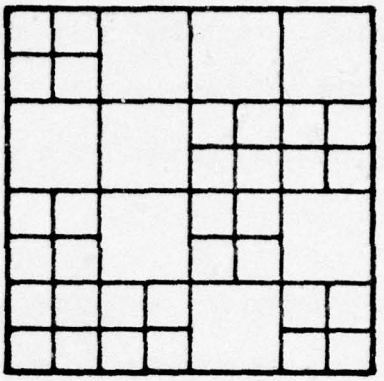

2

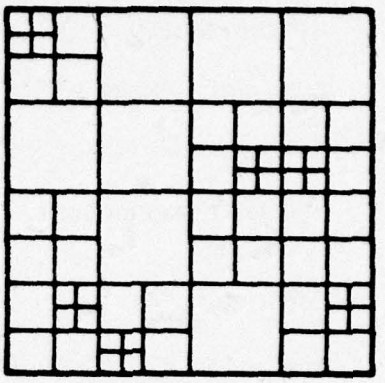

3

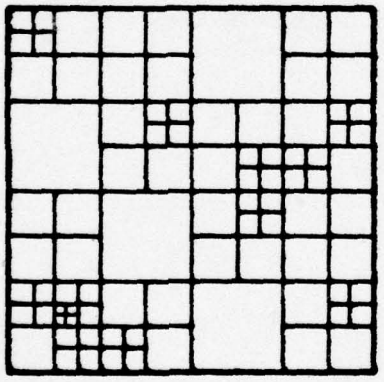

4

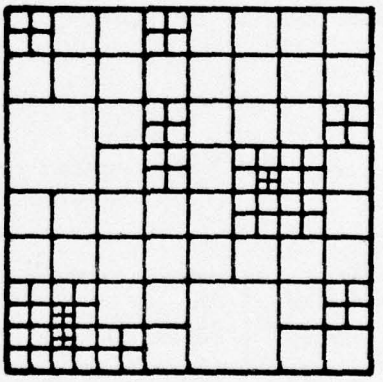

5

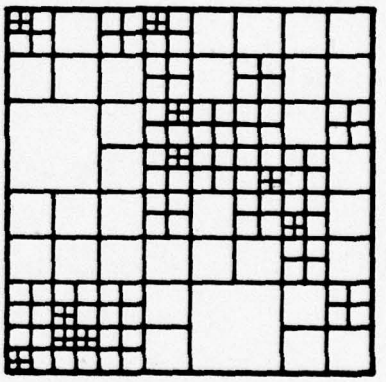

6

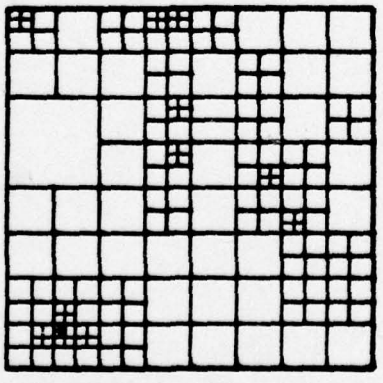

7

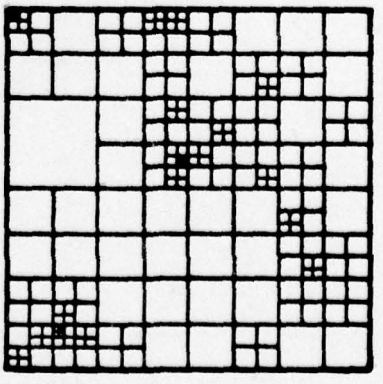

8

FIGURE 3.6

Conjecture 5: The values of the parameters p and σ controlling the degeneracy of the solutions of (3.2), (3.3) and (3.5), (3.6), respectively, do not significantly influence the efficiency index.

Conjecture 6: The adaptive construction of the partitions is effective both for the L_2 and the L_∞-energy norms. The efficiency index for the L_2-norm is better than that for the L_∞-norm, but in both cases it is acceptable.

For problem L and the case L_3 of (3.17), Figures 3.7 and 3.8 show the adaptively constructed meshes for the L_2-energy norm and the L_∞-energy norm, respectively. Tables 3.2 and 3.3 summarize the errors and efficiency indices for these cases. Here the L_∞-energy norm was computed as the maximum value over the set of the four Gaussian points in each element. The table headings are as follows:

(1) Partition identification
(2) Number of degrees of freedom
(3) Number of elements
(4) Square of the error estimator
(5) Square of the exact error
(6) Relative error in percent
(7) Efficiency index

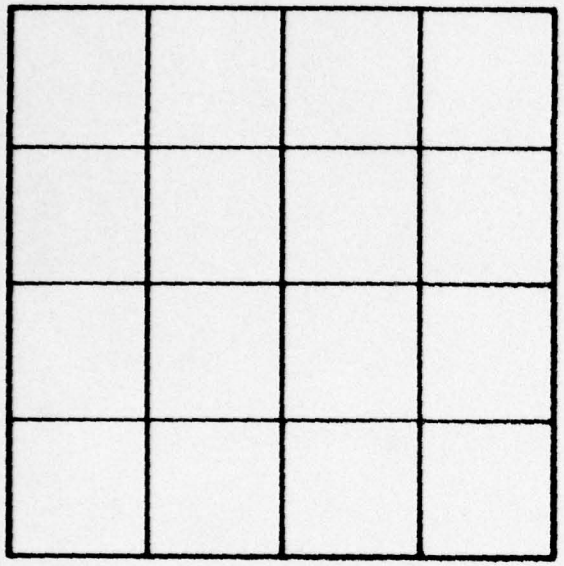

1/4

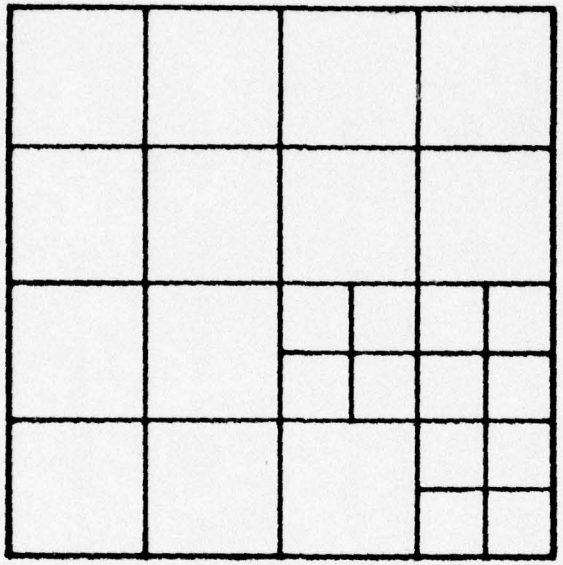

A

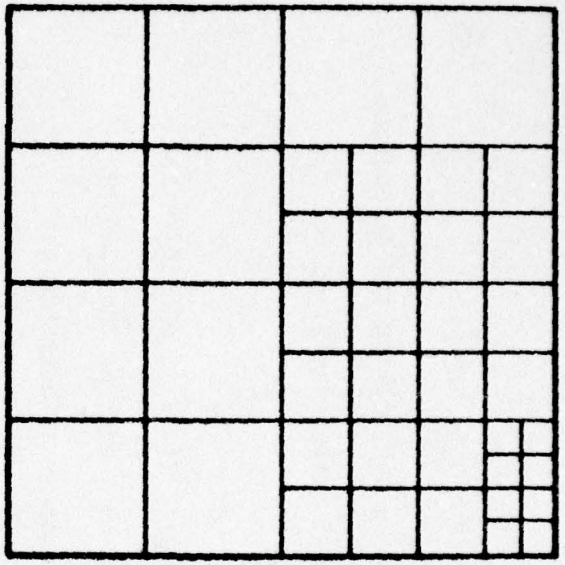

B

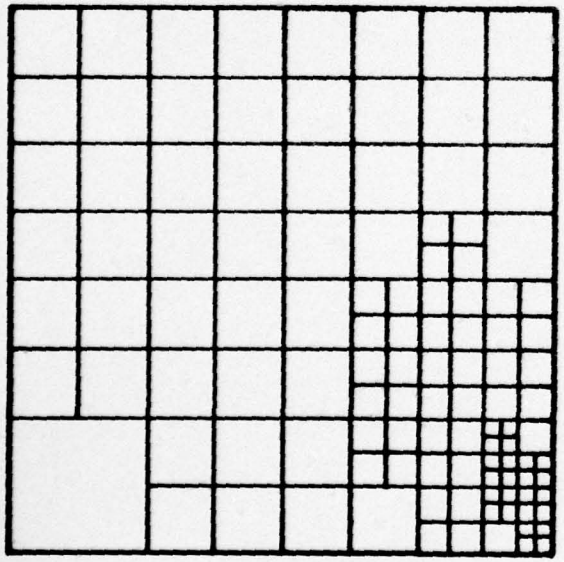

C

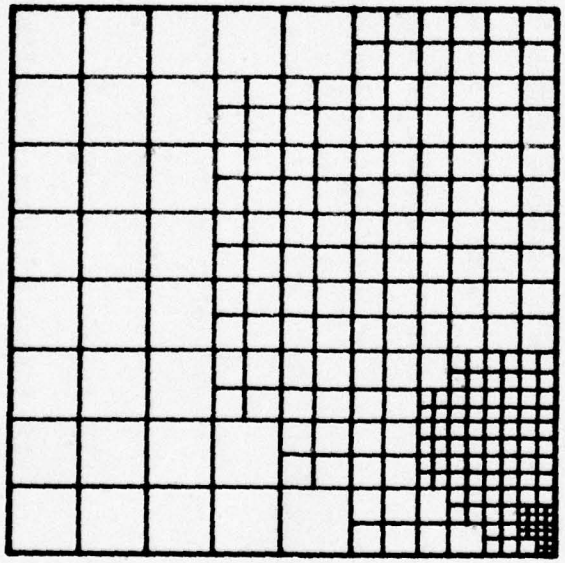

D

ADAPTIVE PARTITION FOR THE L_2-ENERGY NORM

CASE L = t = 1.05, p = 0

FIGURE 3.7

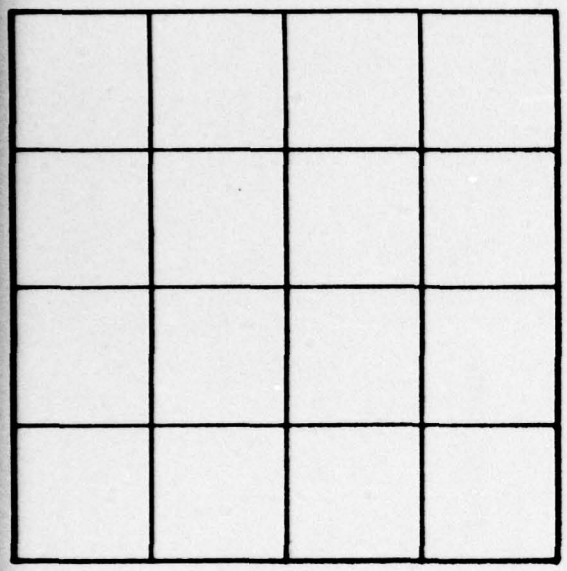

1/4

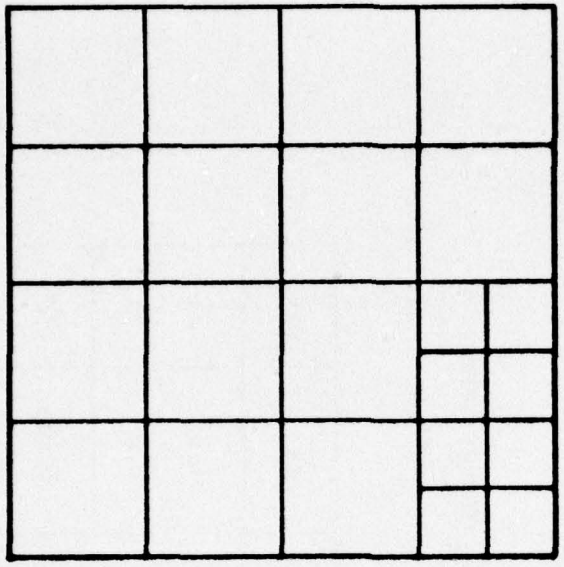

B

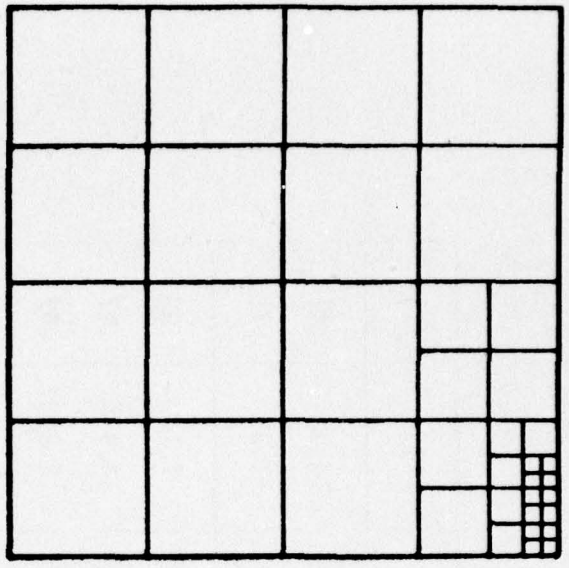

C

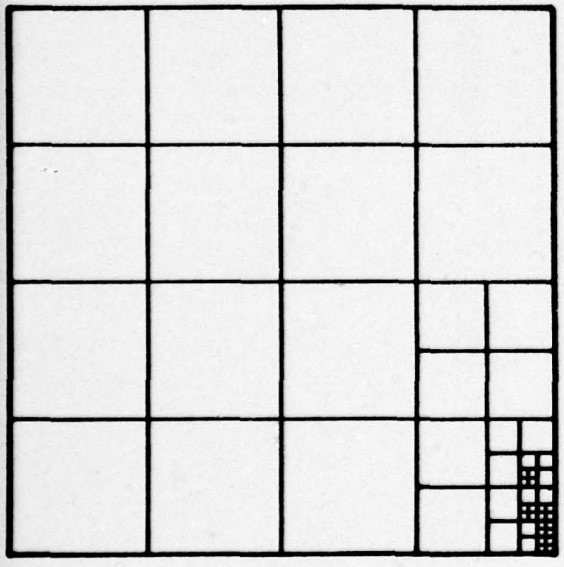

D

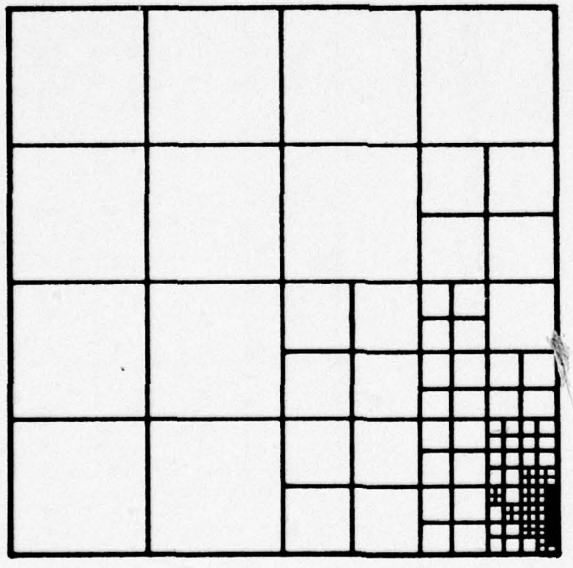

E

ADAPTIVE PARTITION FOR THE L_∞-ENERGY NORM

CASE L■ t=1.05, p=0

FIGURE 3.8

(1)	(2)	(3)	(4)	(5)	(6)	(7)
1/2	1	4	.697(-2)	.155(-1)	19.9%	.67
1/4	9	16	.278(-2)	.535(-2)	11.6%	.72
A	14	25	.158(-2)	.201(-2)	7.16%	.89
B	25	40	.919(-3)	.969(-3)	4.97%	.97
C	86	115	.301(-3)	.319(-3)	2.85%	.97
D	206	250	.137(-3)	.142(-3)	1.91%	.98

Table 3.2 Error estimates for the L_2-energy norm

(1)	(2)	(3)	(4)	(5)	(6)	(7)
1/2	1	4	.119(-1)	.120	31.5%	.31
1/4	9	16	.174(-1)	.122	26.3%	.38
C	20	37	.912(-2)	.155(-1)	6.08%	.77
E	98	139	.142(-2)	.183(-1)	2.01%	.88

Table 3.3 Error estimates for the L_∞-energy norm

4. Adaptive Solution of Linear Problems

4.1 The Basic Design of FEARS.

In recent years, many, often large, general- and special purpose software systems for practical finite element computations have been developed and are used extensively. The same time has brought considerable advances in the theoretical analysis of the method, the development of efficient solution procedures, and the understanding of modern software systems. There appears to be a need for utilizing these and related advances in the design of the next generation of finite element software.

Currently an experimental software system is under development at the University of Maryland at College Park, MD. It has been named FEARS (Finite Element Adaptive Research Solver), and has the following principal design properties.

(i) The system constitutes an applications-independent finite element solver for a particular class of two-dimensional, linear elliptic boundary value problem.

(ii) The problems are defined by a weak mathematical formulation in terms of a bilinear form.

(iii) The a-posteriori error estimates discussed in Chapter 2 above are used to control the reliability of the solution. Different norms may be chosen by the user.

(iv) Adaptive mesh-refinement, based on the error estimates, are to provide for near optimal meshes within a prescribed cost range.

(v) The systems-design takes advantage of some of the natural parallelism and modularity of the finite element method.

The system represents an experimental prototype rather than a production system. Accordingly, extensive provisions for performance evaluation are incorporated in it. A general description of the overall design is given in [7]. A first, preliminary, and, as yet, limited version of the system has been operational for about a year.

As provided by the second design property, the system is based on a weak formulation of the given problem in terms of an appropriate bilinear form B on certain Hilbert spaces H_1, H_2 and a corresponding (load) functional f on H_2. In other words, the underlying mathematical problem is to obtain the (unique) $u_0 \in H_1$ such that

$$B(u_0,v) = f(v), \quad \forall v \in H_2. \tag{4.1}$$

The finite element method then proceeds to the construction of suitable finite-dimensional subspaces $M_1 \subset H_1$, $M_2 \subset H_2$ and the numerical computation of the solution $u(\Delta) \subset M_1$ of

$$B(u(\Delta), v) = f(v), \quad \forall v \in M_2. \tag{4.2}$$

The choice of B and f determines the problem and the structure of the finite element method. The selection of the spaces H_1, H_2 affects the norms used in the error analysis and hence the adaptive control of the overall solution process. Finally, the spaces M_1, M_2 derive from the construction of the particular meshes and the selection of the specific elements. We refer to [8] for the theoretical background of this formulation and to [2] for some of the reasoning behind its use as a basis for the systems-design.

The specific form of B and f used in FEARS may be found in [7]. We note here only that the selected formulation is fairly general. It includes

not only most classical problems and finite element methods but also the elliptic problems of Douglis-Nirenberg type, the forms arising in the use of the least-squares method for first-order systems, various versions of the Lagrange multiplier methods, and many others. Suitable pre-processing facilities can be introduced to simplify the problem definition.

A natural parallel process structure for the system derives from the familiar substructure analysis in engineering design. For this purpose, the domain $\overline{\Omega} \subset R^2$ is defined as the union

$$\overline{\Omega} = \overline{\Omega}_1 \cup \Omega_2 \cup \ldots \cup \overline{\Omega}_N \tag{4.3}$$

of finitely many compact subsets $\overline{\Omega}_i \subset R^2$ which have non-empty interiors Ω_i that are disjoint, $\Omega_i \cap \Omega_j = \emptyset$, $i \neq j$. Each subdomain $\overline{\Omega}_i$ is assumed to be the diffeomorphic image of some fundamental figure F in R^2, (see Figure 4.1). On the intersections of the subdomains these diffeomorphims $\Phi_i : F \to \overline{\Omega}_i$ have to satisfy appropriate compatibility conditions; for details we refer to [7].

The finite element meshes on each $\overline{\Omega}_i$ consist of curvilinear elements which are first defined on F and then mapped by Φ_i into $\overline{\Omega}_i$. Thus the mesh-construction takes place in F. In order to support the adaptive mesh-refinement process, the fundamental figure should admit the definition of a simple hierarchy of partitions consisting of geometrical figures of the same shape, and there should be a simple subdivision algorithm which allows for the construction of the partitions of the hierarchy.

For the design of FEARS the fundamental figure F was chosen to be the closure $\overline{Q}_0$ of the open unit square

$$Q_0 = \{x \in R^2 \mid 0 < x_i < 1, \quad i = 1,2\} \tag{4.4}$$

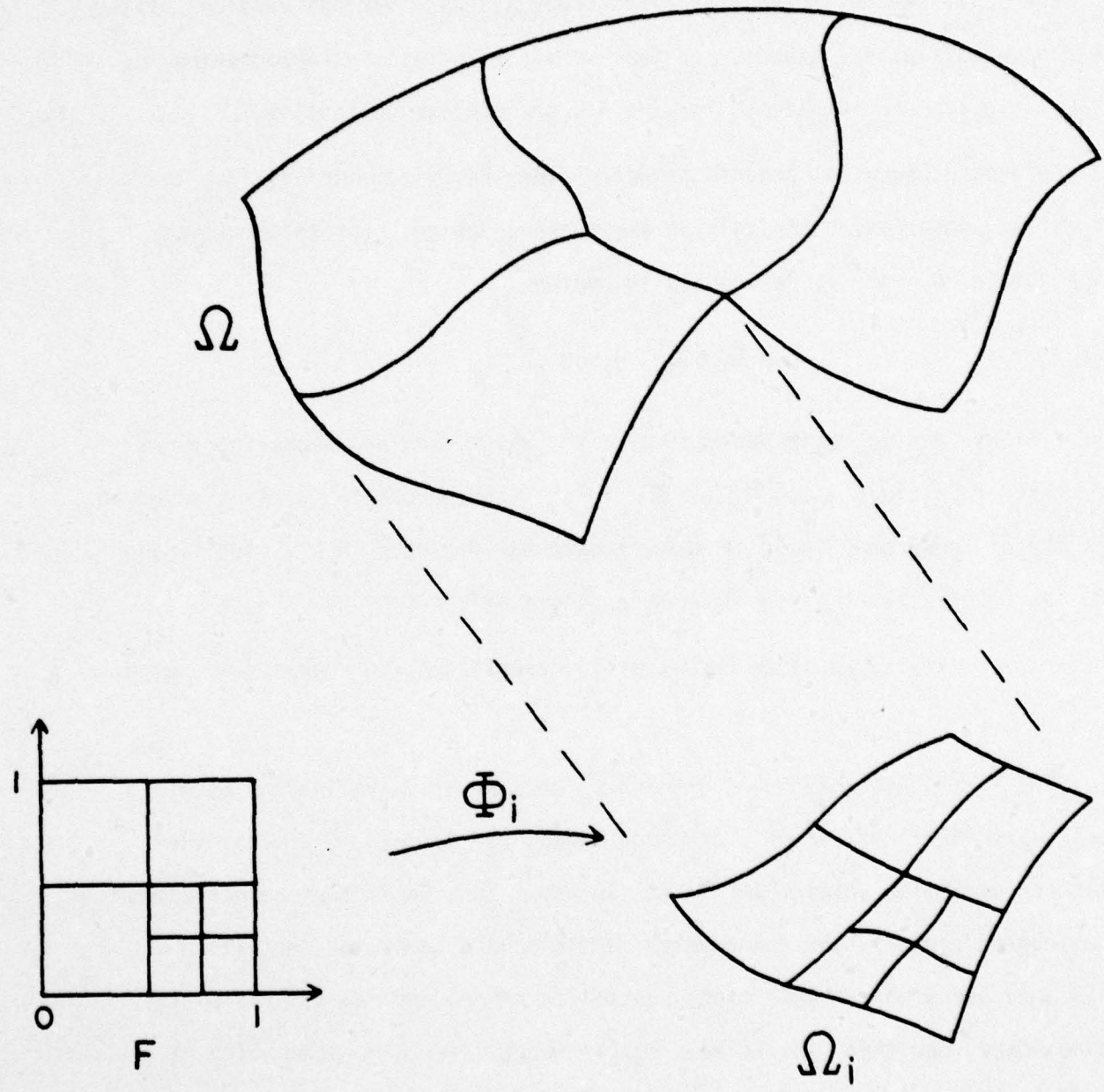

Fig. 4.1

As in the example of Section 3.1, the admissible partitions Δ on $\bar{Q}_0$ are then defined recursively by the two rules (3.8). The current version of FEARS incorporates only bilinear conforming elements on the squares of these partitions of F which are then mapped into the subdomains $\bar{\Omega}_i$. This restriction of the choice of elements was dictated only by limitations of available programming support.

4.2 Computational Aspects

The introduction of parallelism indicated in the design property (v) appears to be a particularly novel aspect of the design of the FEARS system. This parallelism is on the procedural level rather than the instruction-level; that is, it is defined in terms of processes which are autonomous units with their own programs and data. These processes run in parallel and communicate asynchronously in a limited and highly structured manner. A basic design decision was not to store data redundantly whenever possible. Thus each process contains almost all the information needed for it. The use of parallel processes in the design makes it possible to apply multiple processors effectively. But this does not limit the system's use to such specialized architectures; the operating system of a typical large computer simulates parallel processes, and the data segmentation should provide significant advantages.

There are four classes of processes in FEARS, namely, the

(4.5)
(i) geometrical processes
(ii) user processes,
(iii) linear systems solvers, and the
(iv) control process.

Since the closed subdomains $\bar{\Omega}_i$ of (4.3) intersect and hence introduce redundant data, we are led to work exclusively with open subdomains. Accordingly, a separate process is associated with each one of the 2-subdomains $\Omega_1, \ldots, \Omega_N$, with each one of the relatively open, one-dimensional intersections (called 1-subdomains) of two of the Ω_i, and with each 0-dimensional intersections (called 0-subdomains) of several of them. The geometric processes contain all the information relevant to that particular subdomain. This includes the bilinear form, load functional, mapping between Q_0 and the subdomain, boundary conditions where they apply, as well as the current mesh data and associated solution. The only data set stored more than once is the adjacency relation between the subdomains.

A problem is defined by a given domain (4.3), bilinear form B, and associated error norms. Each instance of the system is initialized with a particular problem. It can accommodate several users working simultaneously on this problem, each one with his own boundary conditions, load functional, sequence of meshes, and solutions. The user processes contain the data particular to that user and any information needed for post-processing, graphics, etc.

The third class of processes represent the linear systems solvers which have no permanent data. Finally, the efforts of the various processes are orchestrated by a central control process. It receives commands from the current user, gives commands to the geometric processes and the system solvers, receives reports back from them, and sends reports back to the user.

Basically, after some initialization phase, a user gives a command which tells the system to refine the current mesh, and to compute the corresponding finite element solution so as to achieve a prescribed error tolerance without exceeding a given computational cost.

Hence, if we disregard parallelity for the moment, a user requests the system to execute the following algorithm:

1. [Input] 'initial mesh' Δ; 'tolerances' δ_{abs}, δ_{rel};
   'maximal cost' γ_{max};

2. [Initialization] 'cost' $\gamma := 0$; 'cost increment' $\Delta\gamma := 0$;
   'error estimator' $\varepsilon(\Delta) := \infty$; 'norm' $\nu(\Delta) := \infty$;
   'cut-off parameter' $\bar{\eta} := 0$;

3. [Main Loop]

   While $(\gamma + \Delta\gamma < \gamma_{max})$ and $(\varepsilon(\Delta) > \delta_{abs} + \delta_{rel}\ \nu(\Delta))$ do

   3.1 assemble stiffness equations; compute solution $u(\Delta)$;
   compute norm $\nu(\Delta) = ||u(\Delta)||$; update cost γ;

   3.2 for each element $\tau \in \Delta$ compute error indicator $\eta(\tau)$;
   accumulate estimator $\varepsilon(\Delta)$; if Δ is not the initial mesh
   determine the cut-off parameter $\bar{\eta}$;

   3.3 subdivide each element $\tau \in \Delta$ with $\eta(\tau) \geq \bar{\eta}$; for the
   new elements τ' obtained from τ set $\eta_0(\tau') = \eta(\tau)$;

   3.4 predict cost increment $\Delta\gamma$ of next solution phase.

Briefly, the algorithm continues until either the maximum allotted cost will be exceeded or the error estimator is sufficiently small. Except for the initial mesh the cut-off parameter $\bar{\eta}$ is the maximum value of the quotient $\eta(\tau)^2/\eta_0(\tau)$ where $\eta_0(\tau)$ is the error indicator of the element from which τ was generated by subdivision. This represents a simple procedure to force the error indicators to be closer together.

In the procedure we should distinguish between the mesh design phase and the computation of the final solution. During the construction of the various intermediate partitions Δ there is no need to spend too much effort on the solutions. It turns out that the sequence of refined meshes is not very much affected if the new solution values are only computed on the newly subdivided portions of the mesh; that is, if on the other parts of the mesh the old solution is retained and, where needed, used as boundary condition. We even found that for two to three passes it is possible to compute the effect of the refinement on each element separately. Thus in FEARS a combination of these types of "short" solution passes is used consistently except on the first two meshes, where complete solutions are needed to start the procedure, and on the final mesh.

So far we disregard the effects of parallelism. Generally, the following parallel activities take place:

(a) Several users perform pre- and post-processing while one user is in the solution phase.

(b) The 2-subdomain processes compute their error indicators in parallel.

(c) The 2-subdomain processes refine their meshes in parallel.

(d) The 2-subdomain processes set-up their blocks of the stiffness matrix in parallel.

(e) The 2-subdomain processes decompose their blocks of the stiffness matrix in parallel and send updates to a system solver process.

(f) During short solution passes, "disjoint" solution sets are computed in parallel.

In connection with the activities (d) and (e) above it should be noted that the macro-stiffness matrix has the form

$$\begin{pmatrix} A_1 & & 0 & C_1 \\ & \ddots & & \vdots \\ 0 & & A_N & C_N \\ C_1^T & \cdots & C_N^T & B \end{pmatrix} \tag{4.6}$$

where each diagonal block corresponds to a 2-subdomain and the blocks $C_1, \ldots C_N$, B of the border contain the data for the 0- and 1-subdomains. Clearly, each 2-subdomain process may perform the following tasks in parallel:

(i) Generate the blocks A_i, C_i and send the corresponding contribution for the block B to a separate solver process.

(ii) Decompose A_i, modify C_i accordingly, and send the resulting modification of B to the solver.

After all 2-subdoamin processes finish these steps, the solver process completes the decomposition of B and now the new solution is obtained in an obvious way. Some modifications, of course, are needed in the case of short solution passes.

The efficiency of the refinement strategy depends critically on the design of the data structure for the meshes. A widely used data structure for finite element computations is based on a list of the nodes each pointing to the elements to which it belongs, and a list of the elements which in turn point to the nodes incident with them. This essentially static structure is not very efficient when mesh refinements are introduced. Instead the recursive definition (3.8) suggests the use of a tree structure that corresponds to the refinement process. The tree structure developed for and used in FEARS is described in [9] and we sketch here only the basic idea.

As discussed before, the mesh construction takes place on the closure of the square (4.4). Hence the tree structure represents the refinement

process on $\overline{Q}_0$ as defined by (3.8). As mentioned in Section 3.1, in the resulting partitions we need to distinguish between regular and irregular nodal points (see Figure 3.1). The nodes of the tree correspond to all regular nodal points and to the center of all undivided squares of the partition. The successor relation on the tree represents the subdivision process. For details we refer to [9]. An example of the resulting tree structure is given in Figure 4.2.

The nodes of the tree carry labels of the form (λ_1, λ_2), $\lambda_1, \lambda_2 = -1, 0, +1$, which permit the retrieval of all needed geometrical information. In fact, as shown in [9], simple algorithms are available to perform the following tasks:

(a) For a given tree-node representing a divided or undivided square s determine -- as far as they exists --

  (a1) the corners of s

  (a2) the midpoints of the sides of s

  (a3) the neighboring squares

(b) For a terminal tree node representing an undivided squares

  (b1) subdivide s and extend the tree

  (b2) compute the elementary stiffness matrix of s

(c) Decompose the block A_i of (4.6) defined by the tree using a natural point order induced by the tree corresponding to nested dissection. Thus there is no need for any renumbering algorithms or special strategies.

In connection with (b2) we should note that a particular square s may have up to three corners that are irregular nodal points of the partition.

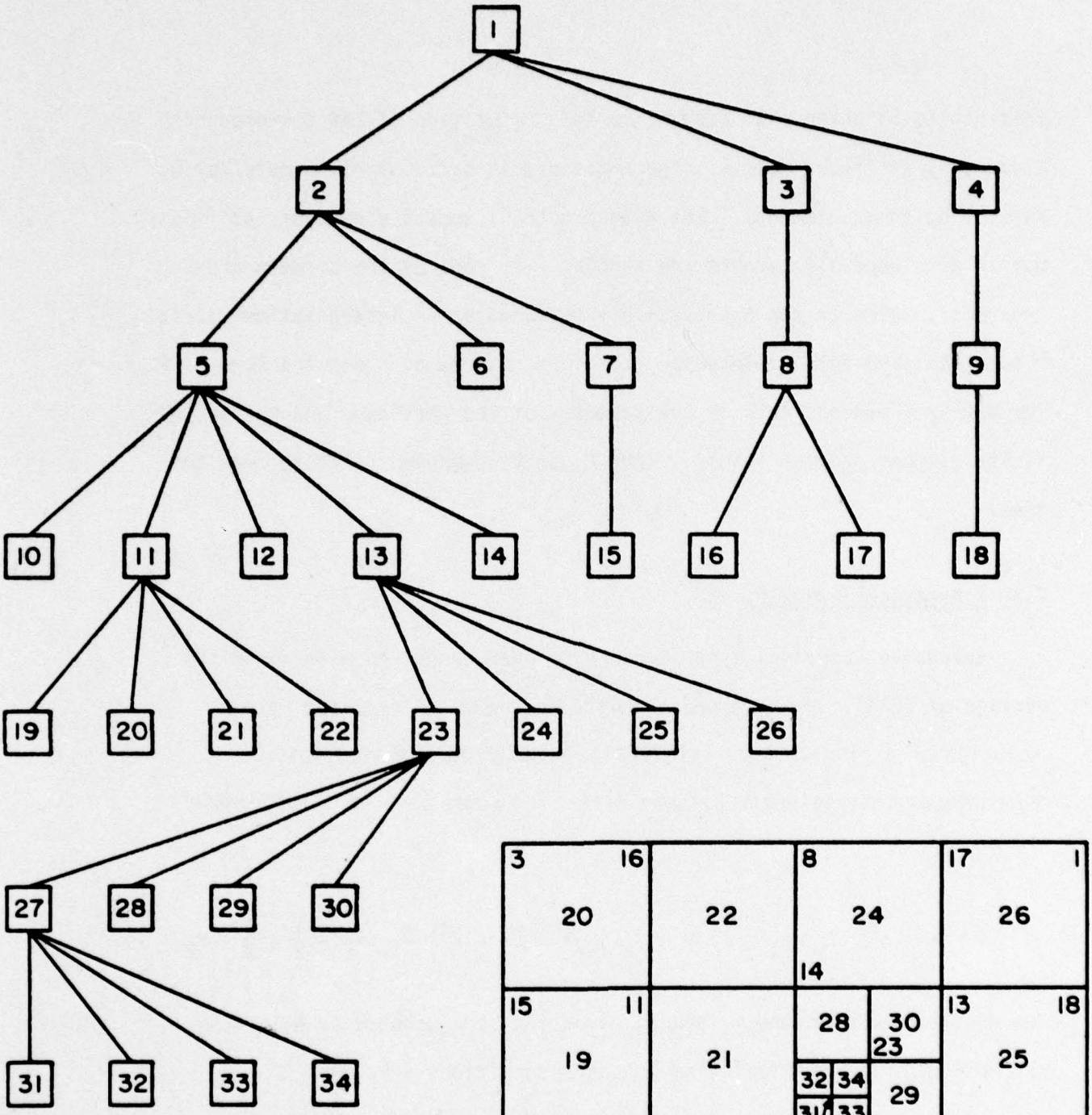
1
2
3
4
5
6
7
8
9
10
11
12
13
14
15
16
17
18
19
20
21
22
23
24
25
26
27
28
29
30
31
32
33
34

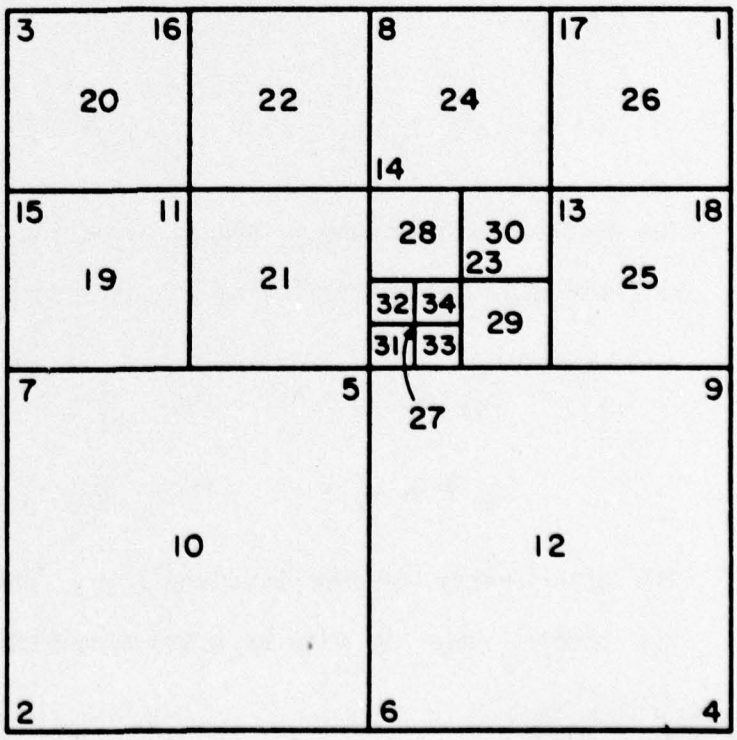
3
16
20
22
8
24
14
17
1
26
15
11
19
21
28
30
23
32
34
31
33
29
13
18
25
7
5
27
9
10
12
2
6
4

Fig. 4.2

This has to be taken into account in the computation of the corresponding elementary stiffness matrix. The procedure is particularly simple for our case of bilinear elements. Let M denote the standard elementary stiffness matrix of s when all corners are regular. If some of the corners are irregular, there exists a -- possibly rectangular -- interpolation-matrix P such that the actual elementary stiffness matrix of s has the form P^TMP. The matrix P depends only on the geometry of the partition and not on the finite element problem itself. Thus P can be computed directly from the tree.

4.3 A Numerical Example

Extensive numerical experiments have been conducted with the pilot version of FEARS. Here we present only one example involving the solution of a plane, linear elasticity problem for an isotropic, homogeneous material with Poisson ratios $\sigma = 0$ and $\sigma = 0.45$. The domain is the L-shaped set

$$\bar{\Omega} = \{x \in R^2 \mid 0 \leq x_1 \leq 1,\ 0 \leq x_2 \leq \tfrac{1}{2}\} \cup \{x \in R^2 \mid 0 \leq x_1 \leq \tfrac{1}{2},\ \tfrac{1}{2} < x_2 \leq 1\}.$$

The displacements in the x_1 and x_2 directions are denoted by u_1 and u_2, respectively, and the following boundary conditions are used

$$u_1 = 0,\ u_2 = +1 \quad \text{for} \quad \tfrac{1}{4} \leq x_1 \leq \tfrac{3}{4},\ x_2 = 0$$

$$u_1 = 0,\ u_2 = -1 \quad \text{for} \quad 0 \leq x_1 \leq \tfrac{1}{2},\ x_2 = 1.$$

The other parts of the boundary, are free of stresses. Thus the problem may be view as a two-dimensional model of an asymmetric

stamp. We note that the singularity of the solution at (1/4, 0), (3/4, 0) introduces oscillatory behavior in the stresses.

The refinement process begins with a coarse regular mesh with step-size $h = 1/4$ (mesh(0)) which is then subdivided into a regular mesh of step size $h = 1/8$ (mesh(1)). For the case $\sigma = 0$ the meshes (2) to (6) generated thereafter by the algorithms are shown in Figure 4.3 and 4.4. Moreover, Figure 4.5 shows the mesh (7) for $\sigma = 0$ as well as the mesh (5) for the case $\sigma = 0.45$ which corresponds to it in the size of the error estimator. (For space reasons the meshes (2), (3), (4) for the case $\sigma = 0.45$ are not included). It is interesting to note the differences in the effect of the singularities for different Poisson ratios at these error tolerances. In all cases the L_2-energy norm was used.

Tables 4.1 and 4.2 show some of the results of these computations

mesh ident.	no of elements	$\varepsilon(\Delta)$	$100\frac{\varepsilon(\Delta)}{\|\|u(\Delta)\|\|_{E,2}}$
1	48	1.073(-1)	10.8%
2	54	9.890(-2)	10.1%
3	66	9.142(-2)	9.3%
4	78	8.389(-2)	8.6%
5	84	7.977(-2)	8.2%
6	111	7.233(-2)	7.4%
7	171	6.071(-2)	6.3%

Table 4.1: "Stamp" problem, Poisson ratio $\sigma = 0$.

mesh ident	no of elements	$\varepsilon(\Delta)$	$100\frac{\varepsilon(\Delta)}{\|\|u(\Delta)\|\|_{E,2}}$
1	48	1.11(-1)	25.2%
2	84	9.43(-2)	21.8%
3	129	8.22(-2)	19.3%
4	183	7.29(-2)	17.2%
5	255	6.60(-2)	15.7%

Table 4.2 "Stamp" problem, Poisson ratio $\sigma = 0.45$

Clearly the relative errors are considerable higher for $\sigma = 0.45$.

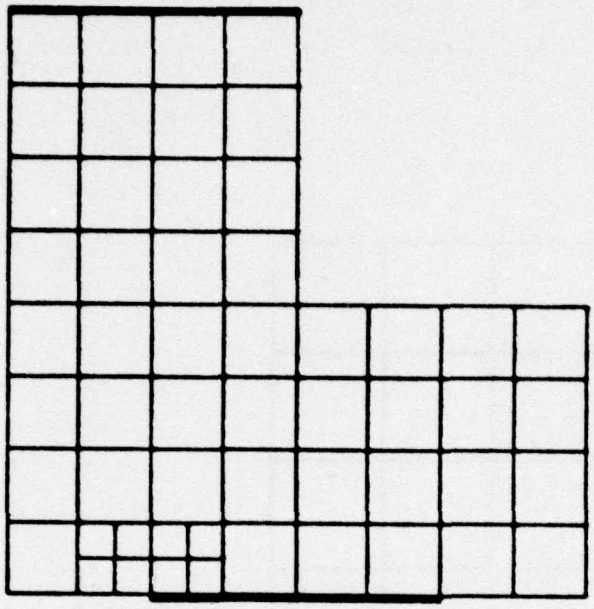

(2)

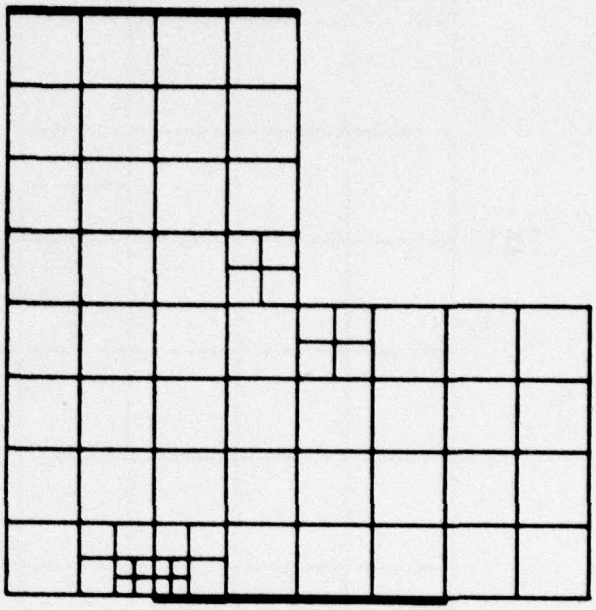

(3)

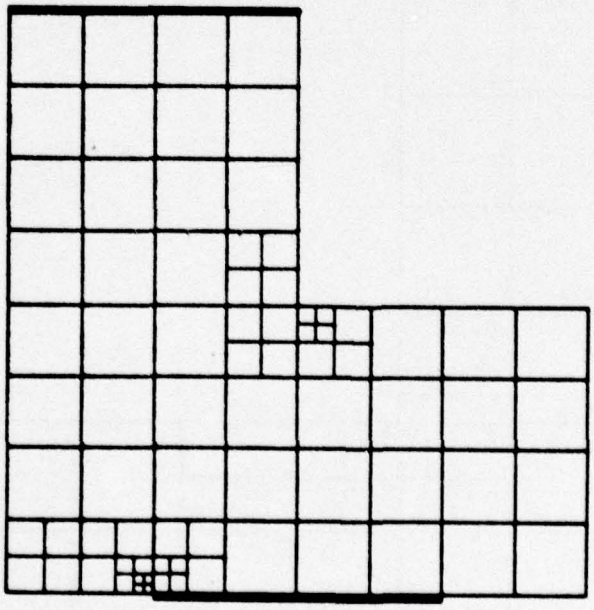

(4)

Fig. 4.3

(5)

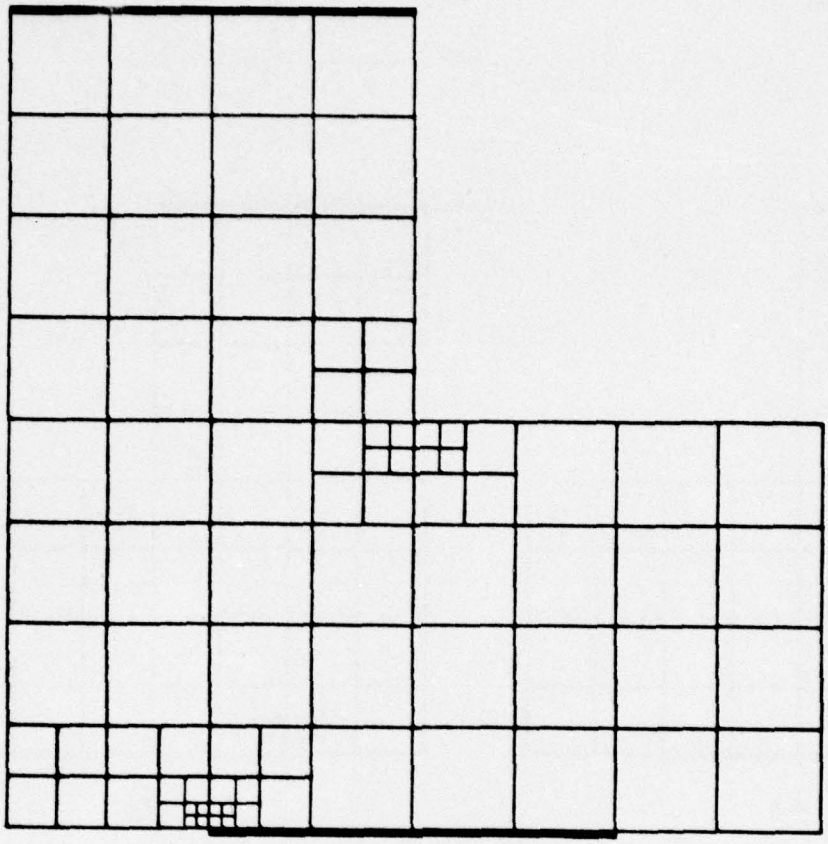

(6)

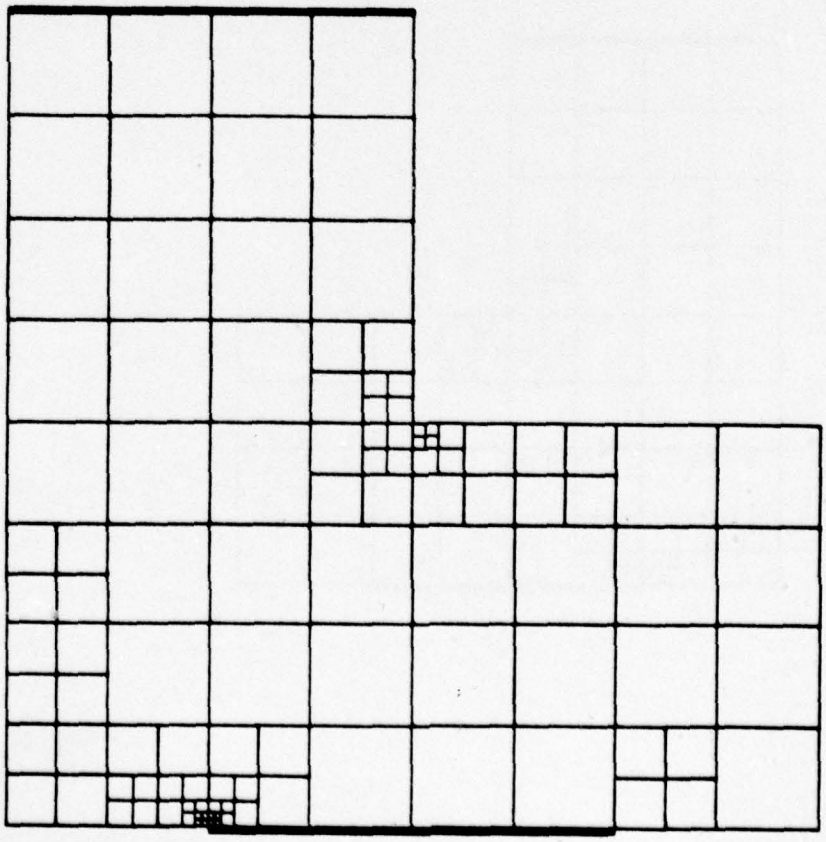

Fig. 4.4

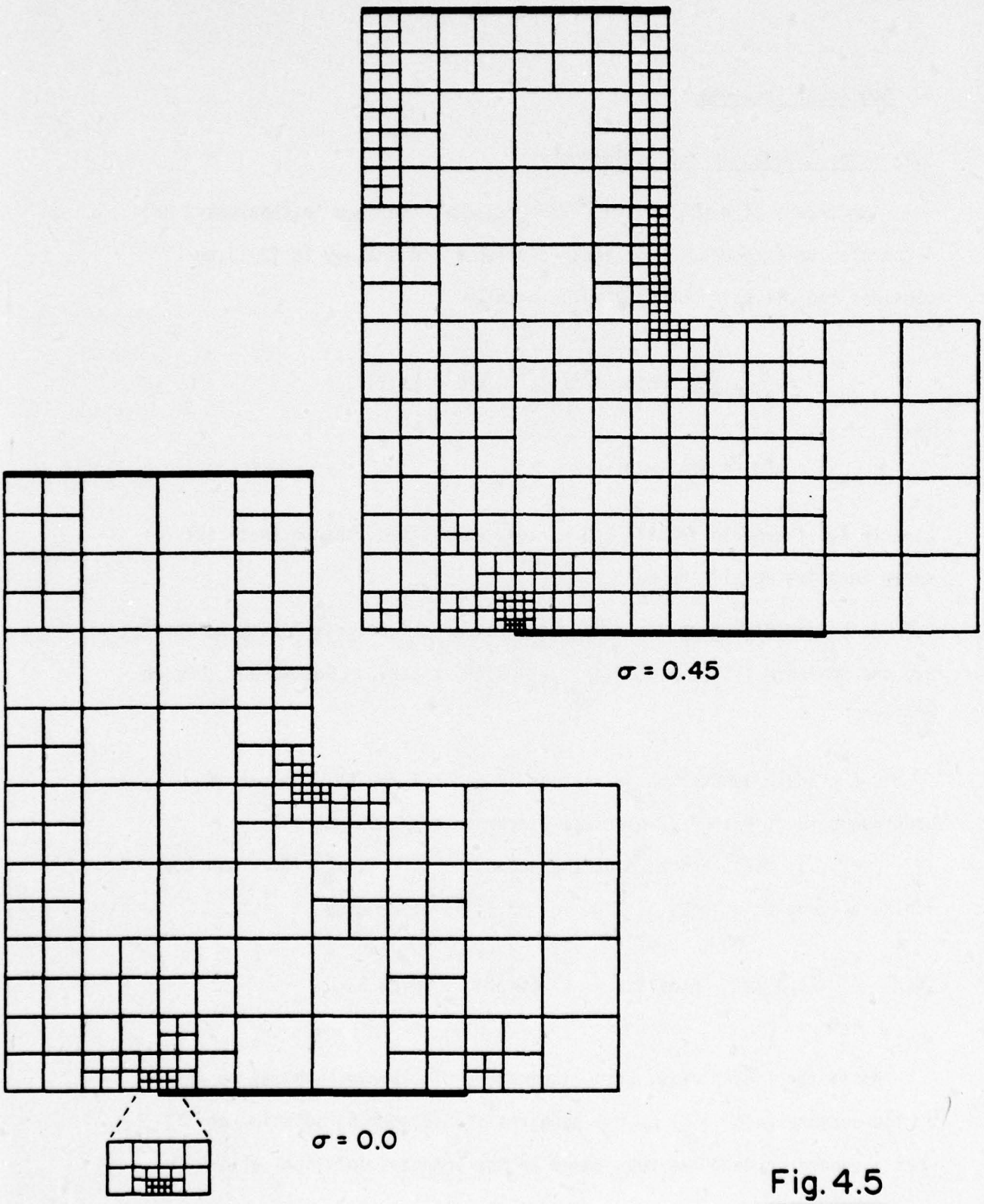

Fig. 4.5

5. Nonlinear Problems

5.1 Error Indicators and Estimators

The theory of a-posteriori error estimates sketched in Chapters 2 and 3 can also be extended to nonlinear problems. In analogy to (2.1) we consider the elliptic boundary value problem

$$-\frac{d}{dx}\, a\left(\frac{du}{dx}\right) + b(u) = f(x), \quad x \in I = [0,1] ,$$

(5.1)

$$u(0) = u(1) = 0.$$

Clearly a,b,f need to satisfy appropriate conditions, but we shall not enter into any details here.

As before different norms may be considered. For simplicity we shall use the seminorm $|u|_{1,p} = ||u'||_{L_p(I)}$ which is here an equivalent norm on $\overset{\circ}{H}{}^1_p(I)$.

Let Δ again denote the partitions (2.6) of I and $\overset{\circ}{S}{}^{\Delta}$ the set of continuous functions on I which are linear on each subinterval I_j^{Δ} , $j = 1,\ldots, m(\Delta)$, and zero at the endpoints $x_0^{\Delta} = 0$, $x_m^{\Delta} = 1$. Then the finite element solution $u(\Delta) \in \overset{\circ}{S}{}^{\Delta}$ of (5.1) is defined by

$$(5.2) \qquad \int_0^1 [a(u')v' + b(u)v]dx = \int_0^1 f(x)v\,dx , \quad \forall v \in \overset{\circ}{S}{}^{\Delta} .$$

As in the linear case, error indicators of various form may be defined on the subintervals I_j^{Δ}. We use here the finite element solution on I_j^{Δ} when a quadratic term has been added to the computed solution $u(\Delta)$. In

other words, set $y_j = u(\Delta)(x_j)$, $j = 0,\ldots, m(\Delta)$ and

$$(5.3)\quad w(x,z) = y_{j-1} + \frac{x - x_{j-1}}{h_j}(y_j - y_{j-1}) + z(x - x_{j-1})(x_j - x),\ \forall x \in I_j^{\Delta}.$$

Then, with the solution $z \in R^1$ of

$$(5.4)\quad \int_{x_{j-1}}^{x_j} a(w_x(x,z))(x_{j-1} + x_j - 2x)dx + \int_{j-1}^{x_j} (b(w(x,z)) - f(x))(x - x_{j-1})(x_j - x)dx = 0,$$

we define the error indicators by

$$(5.5)\quad \eta_j^{\Delta} = |z_j|,\ j = 1,\ldots, m(\Delta),$$

and the error estimator by

$$(5.6)\quad \varepsilon(\Delta) = \begin{cases} \left[\sum_{j=1}^{m(\Delta)} (\eta_j^{\Delta})^p\right]^{1/p}, & 1 \le p < \infty \\ \max_j \eta_j^{\Delta}, & p = \infty \end{cases}$$

Not unexpectedly, (5.4) represents a nonlinear equation for the error indicators. In general, it is easily solvable by standard iterative processes starting with the initial approximation $z = 0$.

The theory of these indicators and estimators is even less developed than, say, in the case of the linear problems of Chapter 3. But under suitable smoothness on a,b,f some of the results of Chapter 2 can indeed by carried over to this nonlinear case. This will be discussed elsewhere.

5.2 Continuation Methods

The equation (5.2) determining the finite element solution $u(\Delta) \in \overset{o}{S}{}^{\Lambda}$ of (5.1) represents a nonlinear system of $n = m(\Delta)-1$ equations in the n unknown $y_j = u(\Delta)(x_j)$, $j = 1,\ldots, n$. In structural analysis the most common technique for solving such systems is the continuation method, (see eg. [10]). For this we assume, for example, that the right side of (5.1) depends on a parameter λ, say, $f(x) = \lambda f_0(x)$ with a given function f_0. Then the resulting system of equations has the form

$$Gy = \lambda g, \quad y \in R^n \tag{5.7}$$

where $G: R^n \to R^n$ is given nonlinear function and $g \in R^n$ a fixed vector. This system (5.7) defines a family of curves $y = y(\lambda)$ in R^n, and the standard continuation approaches numerically trace the solution curve defined by the initial condition $y(\lambda_0) = y^0$ where $Gy^0 = \lambda_0 g$. For example, if $a(0) = b(0) = 0$ then we may take $\lambda_0 = 0$, $y^0 = 0$.

It is well-known that these methods encounter difficulties when the Jacobain $G'(y)$ becomes singular. We have to distinguish here between the potential bifurcation points where rank $(G'(y),-g) < n$ and the limit points where rank $(G'(y),-g) = n >$ rank $G'(y)$. The limit points do not represent intrinsic singularities of our problem. In fact, they loose much of their significance if the solutions of (5.7) are considered as curves in R^{n+1}.

For this we add λ as $(n+1)$st component to the vector y and hence consider, in general, an "underdetermined" equation

$$Fy = c \tag{5.8}$$

involving a function $F:R^{n+1} \to R^n$. A regular C^1-solution of (5.8) is then any curve in R^{n+1} represented by a C^1-parametrization

$$y = y(s), \quad s \in J \subset R^1, \quad y'(s) \neq 0, \quad \forall s \in J \tag{5.9}$$

such that $F(y(s)) = c$ for all s in the open interval J. For arbitrary vectors c in the range of F the resulting collection of curves defines the solution field of F.

An analysis of such solution fields was given in [11] and was used there to show that a particular continuation method is well defined. We shall not enter into details here but sketch only the essential ideas of the approach.

For each vector y in the regularity set

$$R(F) = \{y \in R^{n+1} \mid \text{rank } F'(y) = n\} \tag{5.10}$$

there exists an unique vector $z \in R^{n+1}$ such that

$$F'(y)z = 0, \quad ||z||_2 = 1, \quad \det \begin{pmatrix} F'(y) \\ z^T \end{pmatrix} > 0 \tag{5.11}$$

Hence the tangent mapping

$$T:R(F) \to R^{n+1}, \quad Tx = z \tag{5.12}$$

is well-defined. In [11] the following result was proved:

Theorem 5.1: Let $F:R^{n+1} \to R^n$ be twice continuously differentiable. Then the tangent mapping T of (5.12) is Lipschitzian on any compact subset of $R(F)$, and for any $y^0 \in R(F)$ and $c = Fy^0$ there exists a unique, simple, regular C^1-solution in $R(F)$ of $Fy = c$ which has no endpoint in $R(F)$.

These C^1-solutions in $R(F)$ may be parametrized by the solutions (5.9) of the autonomous initial value problem

$$y' = Ty, \quad y(0) = y^0, \tag{5.13}$$

in which case the parameter is the arclength.

The vector Ty represents the tangent of the solution field at the point $y \in R(F)$ and y is a limit point with respect to the ith variable if $(Ty)_i = 0$. If y is not a limit point with respect to the jth variable then the solution $z \in R^{n+1}$ of the linear system

$$\begin{pmatrix} F'(x) \\ (e^j)^T \end{pmatrix} z = e^{n+1} \tag{5.14}$$

is a multiple of Ty. This provides a simple means for the computation of Ty.

Essentially all numerical continuation methods now are of the predictor-corrector type. In other words, information on an already computed portion of the curve is used to calculate a suitable extrapolation approximating a further curve-segment. Some point on this extrapolating curve is then chosen as the starting point for a corrector-iteration designed to converge to a point on the solution curve.

A general system has been developed for the computation of the C^1-solution of (5.8) through a given starting point. It uses an Euler predictor and Newton's method as corrector. The general scheme of the process may be described as follows:

1. [Input] 'starting point' $y \in R(F)$;

   j:='index such that $(Ty)_j \neq 0$'

2. 'From (5.15) calculate tangent vector' Ty
3. j:= 'index such that $|(Ty)_j| = \max_{i=1,\ldots,n+1} |(Ty)_i|$'
4. 'predict steplength' h
5. 'compute Euler point' z:=y + hTy; 'right side' β;
6. 'apply corrector iteration to Fz = c, $(e^j)^T z = \beta$';
   normal return: y:='final iterate'; go to 7;
   error return: h:=h/2; go to 5;
7. if 'further step required' then go to 2

Let $y^i \approx y(s_i)$, $i = 0,\ldots, k$, $k \geq 1$, be the approximations of the desired solution $y = y(s)$ computed by this process. For the steplength estimation at y^k we consider the quadratic interpolant

$$p(s) = y^k + (s - s_k)Ty^k + (s - s_k)^2 w^k$$

(5.15)

$$w^k = \frac{1}{h_k^2}(y^{k-1} - y^k + h_k Ty^k), \; h_k = ||y^h - y^{h-1}||_2$$

with $p(s_k) = y^k$, $p'(s_h) = Ty^k$, $p(s_{k-1}) = y^{h-1}$. Then it can be shown that

(5.16) $$||y(s_k + h) - p(s_k + h)||_2 \leq h^2 ||w^k||_2 + O(h^3), \quad \text{as } h \to 0.$$

For a given tolerance $\varepsilon > 0$ this suggest the use of the asymptotic steplength formula.

(5.17) $$h = \min\left(\sqrt{\frac{\varepsilon}{||w^k||_2}}, h_{max}\right)$$

In our system, ε is adaptively computed as $\varepsilon = \theta\rho$ using a "safe" convergence

radius p of the corrector iteration and a suitable factor $0 < \Theta < 1$, (see eg. [12]). Figure 5.1 shows this schematically. For further details, we refer to [11].

5.3 A Numerical Example

We consider the boundary value problem (5.1) with the coefficient functions

$$a(s) = \frac{s}{1+s}, \quad -1 < s < \infty ; \; b(s) \equiv 0, \; s \in R^1,$$

(5.18)
$$f(s) = \begin{cases} \lambda & \text{for } \frac{1}{4} < s < \frac{3}{4}, \; \lambda \geq 0, \\ 0 & \text{otherwise} \end{cases}$$

This may be viewed as a model of a one-dimensional rod of lenght one which is clamped at the endpoints and subjected to a load in the direction of its axis. Then λ represents a measure of this load.

In this special case, the exact solution of (5.1) for $\lambda > 0$ turns out to be

(5.19)
$$u(x) = \begin{cases} \alpha\bar{\alpha}x & , \; 0 \leq x \leq \frac{1}{4}, \\ \frac{1}{4}\bar{\alpha} - x + \frac{1}{\lambda}\ln(1 + \lambda\bar{\alpha}(x - \frac{1}{4})) & , \; \frac{1}{4} \leq x \leq \frac{3}{4}, \\ \bar{\alpha}(\alpha - \frac{1}{2}\lambda)x + \frac{1}{4}\bar{\alpha}(1 - \frac{1}{1 + \frac{1}{2}2\lambda}) + \frac{1}{\lambda}\ln(1 + \frac{1}{2}\bar{\alpha}\lambda) & , \; \frac{3}{4} \leq x \leq 1, \end{cases}$$

where $\bar{\alpha} = 1/(1 - \alpha)$ and $\alpha = a(u'(0))$ is the solution of

(5.20)
$$\frac{1}{4}\bar{\alpha}(1 + \frac{1}{1 + \frac{1}{2}\bar{\alpha}\lambda}) + \frac{1}{\lambda}\ln(1 + \frac{1}{2}\bar{\alpha}\lambda) = 1.$$

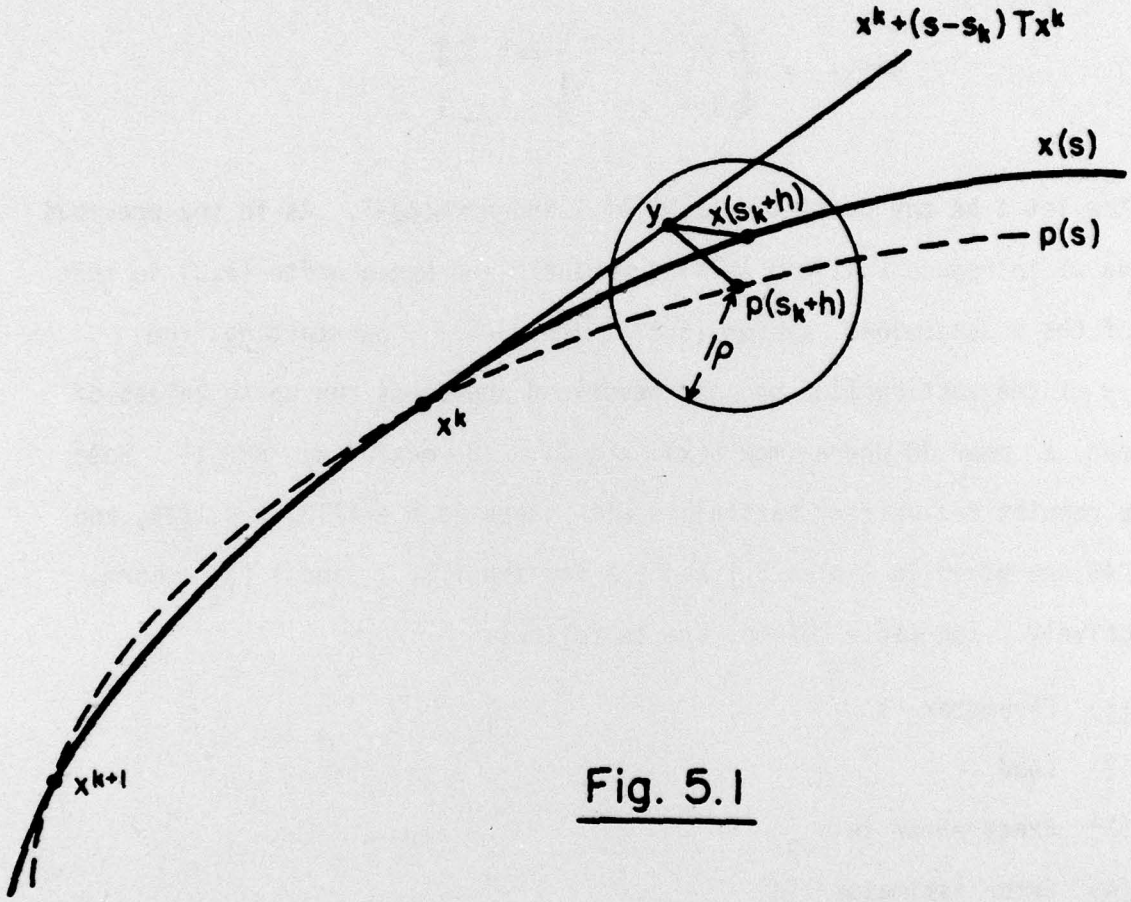

Fig. 5.1

Thus we have here

$$0 \leq u(x) \leq u^*(x), \quad 0 \leq x \leq 1, \tag{5.21}$$

where the limiting function u^* is given by

$$u^*(x) = \begin{cases} 3x, & 0 \leq x \leq \frac{1}{4}, \\ 1-x, & \frac{1}{4} \leq x \leq 1. \end{cases} \tag{5.22}$$

Now let Δ be any partition (2.6) of I and $n = m(\Delta)-1$. As in the previous section we introduce λ as the (n+1)st variable and hence write (5.2) in the form of the undetermined system (5.8) (with $c = 0$). Now starting from $s = 0$, $y = 0$ the continuation process described above was run up to values of the load λ near 30 where $\max\{u(x), x \in I\} > .8 \max\{u^*(x), x \in I\}$. Some of the results for uniform partitions with stepsize $h = 1/12$, $h = 1/24$, and $h = 1/48$ are given in Tables 5.1 and 5.2 for the $|.|_{1,2}$ and $|.|_{1,\infty}$ norm, respectively. The table columns are as follows:

(1) Parameter s

(2) Load λ

(3) Exact error $|e|_{1,p}$

(4) Error estimator $\varepsilon(\Delta)$

(5) Relative error in perant, $100 \cdot |e|_{1,p} / |u_0|_{1,p}$

(6) Efficiency index Θ

$h = 1/2$

(1)	(2)	(3)	(4)	(5)	(6)
0	0	0	0	0	0
.5000	.4880	.8336(-2)	.8334(-2)	8.41%	1.00
1.996	1.955	.3502(-1)	.3462(-1)	9.39%	.989
3.997	3.936	.7339(-1)	.6854(-1)	11.3%	.934
6.000	5.931	.1077	.9102(-1)	12.9%	.846
12.02	11.94	.1695	.1030	14.9%	.608
18.02	17.94	.1936	.9133(-1)	15.1%	.472
24.02	23.94	.2018	.7880(-1)	14.8%	.390
30.02	29.94	.2032	.6848(-1)	14.3%	.337

$h = 1/24$

(1)	(2)	(3)	(4)	(5)	(6)
0	0	0	0	0	0
.4997	.4767	.4072(-2)	.4073(-2)	4.20%	1.00
1.993	1.912	.1720(-1)	.1715(-1)	4.70%	.997
3.994	3.873	.3715(-1)	.3645(-1)	5.78%	.981
6.000	5.863	.5695(-1)	.5387(-1)	6.84%	.946
12.03	11.88	.1014	.8049(-1)	8.92%	.794
18.04	17.89	.1260	.8359(-1)	9.86%	.663
24.04	23.89	.1395	.7931(-1)	10.2%	.568
30.04	29.89	.1469	.7332(-1)	10.4%	.499

h = 1/48

(1)	(2)	(3)	(4)	(5)	(6)
0	0	0	0	0	0
.4996	.4564	.1934(-2)	.1949(-2)	2.08%	1.01
1.987	1.835	.8231(-2)	.8225(-2)	2.33%	.999
3.986	3.753	.1809(-1)	.1801(-1)	2.88%	.995
5.997	5.730	.2846	.2804(-1)	3.46%	.985
12.07	11.77	.5504(-1)	.5065(-1)	4.86%	.920
18.08	17.78	.7331(-1)	.6133(-1)	5.74%	.837
24.08	23.78	.8581(-1)	.6503(-1)	6.30%	.758
30.08	29.78	.9446(-1)	.6520(-1)	6.66%	.690

Table 5.2: "Rod" Problem, $|.|_{1,2}$ -norm, h = 1/12, h = 1/24, h = 1/48

h = 1/12

(1)	(2)	(3)	(4)	(5)	(6)
0	0	0	0	0	0
.4999	.4880	.2513(-1)	.2465(-1)	19.9%	.981
1.996	1.955	.1663	.1488	31.8%	.895
3.997	3.936	.4793	.3571	48.9%	.745
6.000	5.931	.8323	.5047	63.3%	.606
12.02	11.94	1.679	.5974	89.7%	.356
18.02	17.94	2.195	.5343	103%	.243
24.02	23.94	2.527	.4627	110%	.183
30.02	29.94	2.755	.4029	114%	.146

h = 1/24

(1)	(2)	(3)	(4)	(5)	(6)
0	0	0	0	0	0
.4998	.4767	.1237(-1)	.1226(-1)	10.0%	.991
1.993	1.912	.8539(-1)	.8088(-1)	16.7%	.947
3.994	3.873	.2677	.2308	27.6%	.862
6.000	5.863	.5024	.3860	38.5%	.768
12.03	11.88	1.184	.6401	63.4%	.541
18.04	17.89	1.685	.6806	78.8%	.404
24.04	23.89	2.045	.6517	88.9%	.319
30.04	29.89	2.310	.6054	96.0%	.262

h = 1/48

(1)	(2)	(3)	(4)	(5)	(6)
0	0	0	0	0	0
.4996	.4564	.5906(-2)	.5879(-2)	5.01%	.996
1.987	1.835	.4119(-1)	.4015(-1)	8.39%	.975
3.986	3.753	.1367	.1273	14.5%	.931
5.997	5.730	.2732	.2397	21.2%	.878
12.07	11.77	.7398	.5308	39.8%	.717
18.08	17.78	1.148	.6795	53.8%	.592
24.08	23.78	1.478	.7371	64.3%	.499
30.08	29.78	1.745	.7478	72.6%	.429

Table 5.2: "Rod" Problem, $|.|_{1,\infty}$ norm, h = 1/12, h = 1/24, h = 1/48

For small λ the error decreases again linearly with h. For larger λ the errors are still very large and the asymptotically expected convergence has not yet set in. As in the linear case, the efficiency index improves with decreasing relative error and Θ is close to one already for errors of the order of 5%. Not unexpectedly, the errors in the $|.|_{1,\infty}$ norm are much worse than in the $|.|_{1,2}$ norm but for reasonable errors the efficiency index is again close to one.

Clearly the results in these tables are practically useless for higher values of λ. We would need considerably smaller step sizes h to get acceptable relative errors for large λ. In order to reduce the resulting very heavy computational cost, we need to use once again adaptive mesh constructions.

For this we apply, as in the linear case, the principal of equilibration of the error-indicators. Thus, for any fixed λ all those subintervals I_j are subdivided for which the error-indicator exceeds a certain cut-off value $\overline{\eta}$. On the new partition an approximate solution is obtained by interpolation and then corrected by means of a few Newton-iteration steps. Now the continuation process is applied again until a further refinement becomes necessary.

There are as yet numerous open questions about this combination of continuation and adaptive mesh refinement. But as Table 5.3 and Figure 5.2 show, the process is highly effective.

n	s	λ	$\lvert e\rvert_{1,2}$	$\varepsilon(\Delta)$	$100\frac{\lvert e\rvert_{1,2}}{\lvert u_0\rvert_{1,2}}$	Θ
3	0	0	0	0	0	0
	.5000	.4959	.2535(-1)	.2524(-1)	25.2%	.996
	1.999	1.985	.1016	.9331(-1)	26.9%	.919
	3.999	3.977	.1887	.1358	28.8%	.720
5	3.999	3.977	.7371(-1)	.6952(-1)	11.3%	.950
	5.996	5.967	.9464(-1)	.8463(-1)	11.3%	.894
	7.997	7.966	.1138	.9400(-1)	11.7%	.826
7	7.997	7.966	.6137(-1)	.5658(-1)	6.32%	.922
	9.996	9.962	.6188(-1)	.5690(-1)	5.81%	.920
	12.00	11.96	.6297(-1)	.5764(-1)	5.53%	.915
	18.00	17.96	.6863(-1)	.6052(-1)	5.36%	.882
8	18.00	17.96	.5205(-1)	.4748(-1)	4.07%	.912
	20.00	19.96	.5177(-1)	.4717(-1)	3.95%	.911
	22.00	21.96	.5172(-1)	.4702(-1)	3.89%	.909
	28.00	27.96	.5256(-1)	.4711(-1)	3.75%	.896
9	28.00	27.96	.4244(-1)	.3855(-1)	3.02%	.908
	30.00	29.96	.4184(-1)	.3803(-1)	2.95%	.908

Table 5.3: "Rod" Problem, Adaptive Mesh Construction, $\lvert . \rvert_{1,2}$ norm.

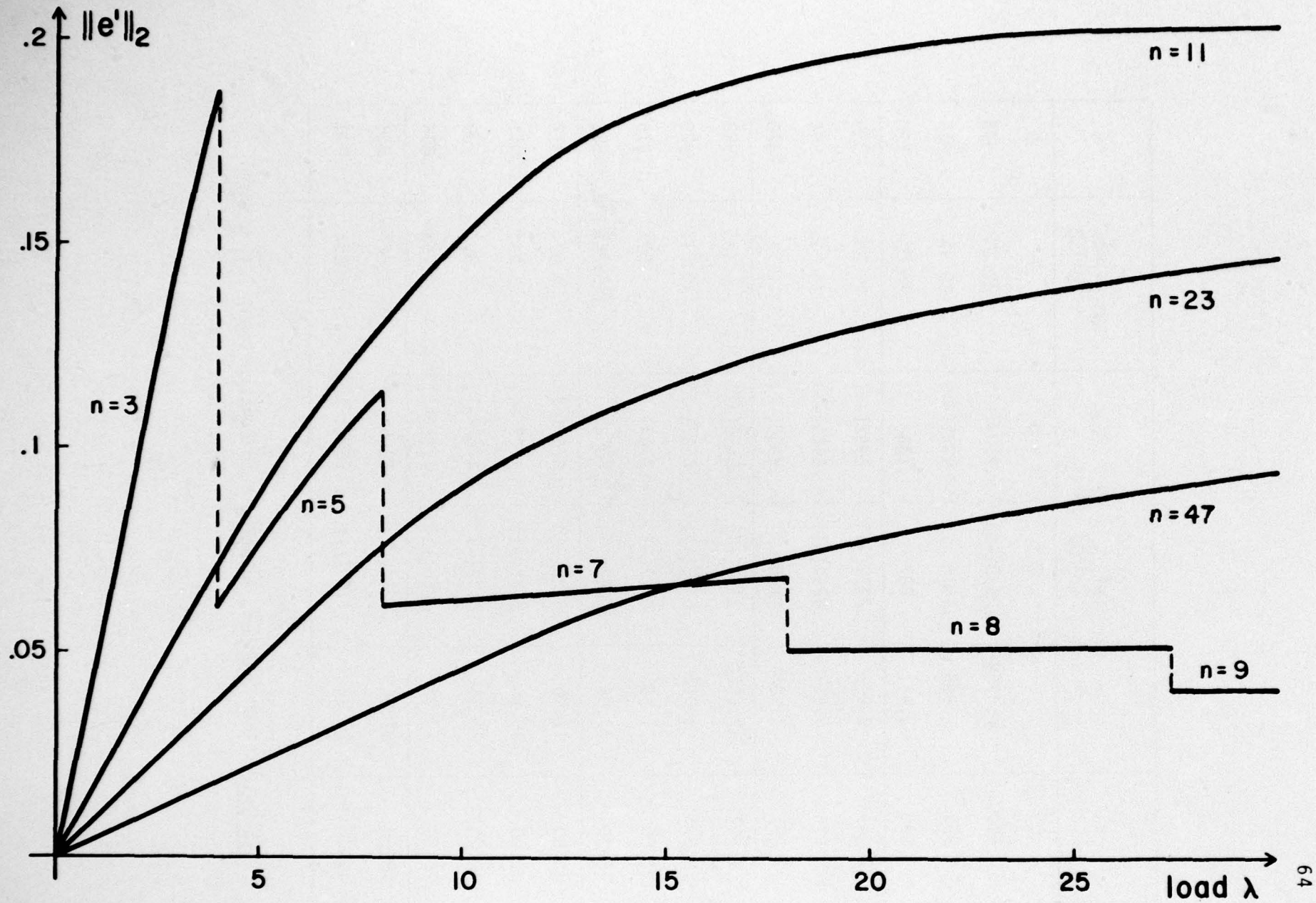

Fig. 5.2

6. Conclusions

Although much work still needs to be done, we believe that the approaches presented here can provide satisfactory answers to the two questions (1.1) raised in the introduction. We summarize briefly some of the conclusions that can be drawn from our results:

a) The a-posteriori error estimates provide reliable information for a wide class of problems and under a variety of different norms.

b) In all our experience, the estimates are acceptable even for relative errors of about 5-10% and they improve with decreasing errors.

c) In the one-dimensional case the theory of the a-posteriori estimates is rather well established but in the two-dimensional and even more so in the nonlinear case there are still a number of open theoretical questions.

d) The error estimates provide a very effective means for controlling the adaptive construction of near-optimal meshes.

e) Experience has shown that the errors for the adaptively constructed meshes show near-optimal character even in the presence of severe singularities.

f) Adaptive mesh construction generally provides an overall savings in computational cost and improves the efficiency index of the error estimates.

g) For an effective implementation of the adaptive mesh construction special attention needs to be paid to all aspects of data management. A tree structure for the representation of a hierarchy of meshes has proved itself to be very advantageous in this connection and allows also for natural pivoting by nested dissection.

h) Our experience with the FEARS project confirms that general-purpose finite element solvers can be constructed which provide near-optimal solutions within a given cost range.

i) In the design of such finite element solvers it is possible to utilize natural parallelity features of the finite element method and to achieve a natural data segmentation.

j) The a-posteriori error estimates are also very effective for nonlinear problems although the corresponding theory is as yet far from complete.

k) For the solution of nonlinear equilibrium problems of the type arising, for instance, in structural analysis stable continuation processes can be designed which are not affected by limit points.

l) In the case of nonlinear problems, the a-posteriori error estimation and adaptive mesh-construction techniques can be combined with the continuation process with highly advantageous effects on the computational cost and the efficiency indexes of the error estimates.

i) In the design of such finite element solvers it is possible to utilize natural parallelity features of the finite element method and to achieve a natural data segmentation.

j) The a-posteriori error estimates are also very effective for nonlinear problems although the corresponding theory is as yet far from complete.

k) For the solution of nonlinear equilibrium problems of the type arising, for instance, in structural analysis stable continuation processes can be designed which are not affected by limit points.

l) In the case of nonlinear problems, the a-posteriori error estimation and adaptive mesh-construction techniques can be combined with the continuation process with highly advantageous effects on the computational cost and the efficiency indexes of the error estimates.

7. References

[1] I. Babuska, W. Rheinboldt, Computational Aspects of Finite Element Analysis; in "Mathematical Software-III", ed. by J. R. Rice, Academic Press, Inc., New York, 1977, pp. 225-255.

[2] I. Babuska, W. Rheinboldt, Mathematical Problems of Computational Decisions for the Finite Element Method in "Mathematical Aspects of Finite Element Methods" ed. I. Galligani, E. Magenes, Lecture Notes in Mathematics, Vol. 606, Springer Verlag/Germany 1977, pp. 1-26.

[3] R. H. Gallagher, Computerized Structural Analysis and Design -- The Next Twenty Years, Keynote Lecture, Second National Symposium on Computerized Structural Analysis, George Washington University, Washington, D. C., March 1976.

[4] I. Babuska, W. Rheinboldt, Error Estimates for Adaptive Finite Element Computations, SIAM Journal on Numerical Analysis 15, 736-754, (1978).

[5] I. Babuska, W. Rheinboldt, A-Posteriori Error Estimates for the Finite Element Method; International Journal for Numerical Methods in Engineering 12, 1597-1615, (1978).

[6] I. Babuska, W. Rheinboldt, Analysis of Optimal Finite-Element Meshes in R^1; Mathematics of Computation, 33, 146, 1978, in press.

[7] P. Zave, W. Rheinboldt, Design of an Adaptive Parallel Finite Element Systems; ACM Trans. on Mathematical Software, March/June 1979, in press.

[8] I. Babuska, A. K. Aziz, Survey Lectures on the Mathematical Foundations of the Finite Element Method, in "The Mathematical Foundations of the Finite Element Method with Applications to Partial Differential Equations" ed. by A. K. Aziz, Academic Press, New York, 1972, pp. 3-359.

[9] W. Rheinboldt, C. Mesztenyi, On a Data Structure for Adaptive Finite Element Mesh Refinements, University of Maryland, Computer Science Technical Report TR-660, 1978; ACM Trans. on Mathematical Software, submitted.

[10] W. Rheinboldt, Numerical Continuation Methods for Finite Element Applications, in "Formulations and Computational Algorithms in Finite Element Analysis" ed. by J. Bathe, J. T. Oden, W. Wunderlich; MIT Press, Cambridge, Mass. 1977, pp. 599-631.

[11] W. Rheinboldt, Solution Fields of Nonlinear Equations and Continuation Methods, University of Pittsburgh, Institute for Computational Mathematics and Applications, Technical Report ICMA-79-04, March 1979, SIAM Journal Numerical Analysis, submitted.

[12] W. Rheinboldt, An Adaptive Continuation Process for Solving Systems of Nonlinear Equations in "Proc. of the Semester on Mathematical Models and Numerical Methods", Stefan Banach Ctr. Publ. Vol. 3, Polish Academy of Science, Warsaw, Poland 1977, pp. 129-142.